Performance Analysis of a Grid Connected Hybrid Photovolatic and Wind Electricity Generation System in Cold Climate

Dayu Yang

Master's Thesis
Department of Physics, University of Jyväskylä
Master's Degree Programme in Renewable Energy
Supervisor: Dr. Jussi Maunuksela
14 August 2007

Acknowledgements

I would like to express my deepest gratitude to my supervisor and teacher Dr. Jussi Maunuksela, who has inspired me and patiently guided me through the research problems. I would also like to extend my gratitude to Laboratory Engineer Arjo Heinsola, Dr. Hannele Holttinen and Dr. Mohanlal Kolhe for discussions and comments.

I would like to thank Paolo Matelloni, Lea Teiniranta and everyone in the lab for creating a good atmosphere, as well as to all the personnel in the Renewable Energy Programme for your help and share.

Especially, I want to thank my parents, friends for their support and love.

In Jyväskylä, 27 July, 2007.
Dayu Yang

Abstract

A Hybrid Photovoltaic (PV) and Wind Electricity Generation System has been monitered and analyzed over a period of two years at Central Finland in order to examine the behavior of grid-connected hybrid systems in cold climate. The hybrid system contained a 4.16 kW_p PV system, a 10 kW wind turbine, and monitoring system. Over the monitoring period, the total electricity production was 8962.64 kWh of which 56.86 % was generated by PV arrays and 43.14 % by the wind turbine. The monthly electricity production was between 50.79 kWh and 777.57 kWh. For the PV sub-system, the averages of the daily array yield for each array and the system yield were 2.08 h/d, 2.31 h/d, and 2.06 h/d, respectively. Corresponding array and the system efficiencies were 2.79 %, 3.21 %, and 2.78 %, respectively; the array and the system performance ratios were 0.620, 0.714, and 0.618, respectively. The daily average inverter efficiency of two IG 60 inverters were 91.99 % and 92.97 %, respectively. The daily average wind speed was 3.30 m/s which was lower than the turbine's cut-in wind speed, the daily average site turbulence intensity was 0.25. The wind turbine efficiency, capacity factor, and wind availability factor were 0.44, 0.05, and 0.42, respectively.

The monitoring results showed that the grid-connected hybrid system is more reliable than the single renewable resource power system. However, the hybrid system in our case did not offer consistent electricity production in Central Finland region, and the system performance was unsatisfactory. The PV system performance was affected by the mounting fault that caused cracks on the PV modules; the system performance was barely adequate from April to September, and it was affected significantly during the winter months by operation under low insolation condition and snow accumulation. The wind sub-system measurement was unrealiable. The wind turbine was over-sized, and the turbine performance was unsatisfactory due to low wind speed, icing and high turbulence intensity. Small scale wind turbines with battery storage might be suitable in Central Finland region.

Table of Contents

Chapter 1

Introduction

Due to the contradiction between gradual growth of the global energy demand and diminishing fossil fuel resources, renewable energy such as solar energy, wind energy, bioenergy, and hydropower might become a new manner in which we produce energy for sustainable development. Photovoltaic (PV) and wind energy systems are the most promising candidates of the future energy technologies, and it has been widely noticed that grid connected PV and wind energy markets have grown rapidly.

Energy generation system reliability has been considered as one of the most important issues in any system design process. However, natural energy resources are unpredictable, intermittent, and seasonally unbalanced. Therefore, a combination of two renewable energy sources may satisfy bigger share of electricity demand and offer reliable and consistent energy supply. The Hybrid PV and Wind Electricity System is well suited to conditions where sun light and wind have seasonal shifts, for example, in summer the sun light is abundant but windless, while in winter wind resource increased that can complement the solar resource. The reliability of the stand-alone hybrid PV-wind system in producing energy has been proven by earlier studies [1, 2, 3, 4]. However, there are few studies available on the performance of grid-connected hybrid photovoltaic and wind electricity generation systems.

Master's Degree Programme in Renewable Energy (RE) at the University of Jyväskylä is doing research on the multidisciplinary aspects of the renewable energy sector. The RE demonstrations of the programme are focused on distributed energy technologies and includes an integrated renewable energy system for Viitasaari ABC service station and a PV system for Saarijärvi Central School.

A Hybrid Photovoltaic (PV) and Wind Electricity Generation System which contained a 4.16 kW_p PV system and a 10 kW wind turbine with utility grid connection was installed in Viitasaari ABC service station located

in Central Finland, and it started generating electricity in February 2005. However, only a small amount of the electricity demand of the station was generated by the hybrid system. The purpose of this study was to analyze the performance of the hybrid system over a monitoring period of two years. The analysis of the monitoring results from the photovoltaic sub-system was done following the procedures described in Ref. [5]. The wind energy system was analyzed following the procedures described in Ref. [6].

Chapter 2

Theoretical Background

2.1 Definitions

Photovoltaic, or *PV* is a solar power technology to convert energy directly from sunlight into electricity. *Solar cells* or *PV cells* are the devices to produce direct current electricity (DC) from the sun's rays.

Wind power is conversion of wind energy into more useful forms, usually to generate electricity by using wind turbines. A *wind turbine* is a machine for converting the kinetic energy in wind first into mechanical energy then to electricity by a generator.

Any power system that incorporates more than one generator is referred to as a *hybrid power system*. The electric generator could mean, for example, PV array, wind turbine, hydro generator, or diesel, gasoline generators. In our case, a *Hybrid PV and Wind Electricity System (HPWS)* is a power system that contains PV cells and wind turbine to generate electricity.

In general, *Cold* is a relative term, which is defined as having a low temperature and marked by deficient heat. Different people make different sense of cold climate, feeling no warmth; uncomfortably chilled are more common expressions for most people. In this paper, *cold climate* is defined as one in which snow, ice, freezing temperature, dark winters and long summer days are considerations in the design and operation of a HPWS. [7]

2.2 Specific site condition of HPWS

Unpredictable, intermittent natural energy resources and the seasonal unbalance of the energy resources are the most important reasons to install a hybrid renewable energy supply system. The HPWS provides a more reliable and stable energy supplement. In Ref. [8] is summurized where the HPWS

should be considered:

- Average electricity demand is moderate or large (larger than 30 W in cold climates);
- Winter time solar insolation is much lower than the summer time insolation;
- Reliable wind resource is available during the dark winter;
- The operating and maintenance requirements of the PV and wind system can be satisfied at a reasonable cost.

The system can be categorized by the energy storage methods:

- Batteries are usually used for energy storage in remote location where it is inconvenient or expensive to use conventional grid to supply electricity.
- The utility grid is used in the rest of locations as storage devices and backup power.

In this paper, we focus on the cold climate issues related to HPWS with grid connection. The site conditions should fulfill the installation and operation requirements for both the PV array and the wind turbine. For the PV array, a true south direction without any obstacles facing the sun is needed. For the wind turbine, appropriate wind speed and wind direction are key elements to the whole system, and the turbine should be mounted into non-turbulent wind higher than trees and without other obstacles. Enough space is needed to site the PV modules, wind turbine tower, and also to properly anchor the guy wires.

2.3 HPWS components

A typical grid connected Hybrid PV and Wind Electricity System (HPWS) contains PV array, wind turbine, balance of the system (BOS) and the utility grid. PV array and wind turbine are the core components of the HPWS as energy generator. The utility grid acts as energy storage function as well as backup supplement. The term 'balance of the system' refers to all of the system components except the renewable generator and the grid, it generally contains conversion devices such as DC-AC inverter, the PV mounting and wind turbine tower, monitoring system and safety equipments.

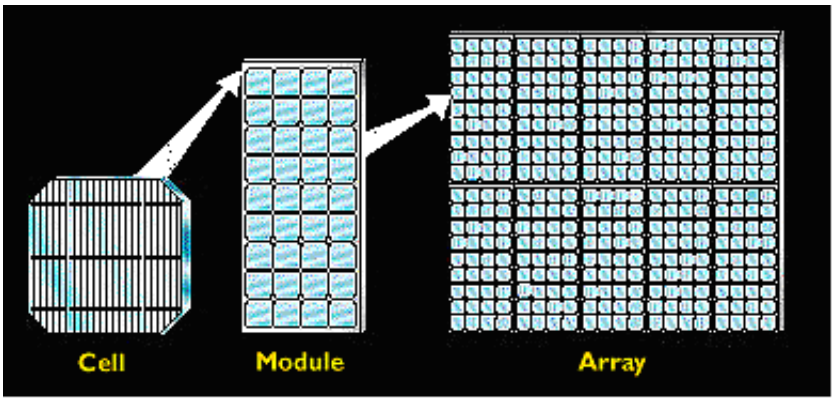

Figure 2.1: Conceptual relationship between the PV cell, module and array

2.3.1 Photovoltaics

Photovoltaic cells are made of semi-conducting materials and the most commonly used material is silicon. When sunlight is absorbed by these materials, the solar energy knocks electrons loose from their atoms, allowing the electrons to flow through the material to produce electricity. [8, 9]

A single PV cell typically produces a small amount of power and in order to increase the operating voltage, the cells are connected in series to form a PV module. A photovoltaic array consists of a number of electrically connected PV modules, which can be connected together in series to generate a higher voltage or in parallel to get a higher current. Fig 2.1 shows the conceptual relationship between the PV cell, module and array. [10]

Solar photovoltaic technologies are developed by many research institutes. The first and second generation's photovoltaic cells, for example, crystalline silicon, crystalline III-V, polycrystalline and amorphous thin films are in wide commercial use. Next generation of the PV cells is already on the laboratories research benches. Organics, nanotechnologies, multi-multiple junctions, band gap engineering, thermo-tuned concepts—all of these new technologies are aimed either for a high efficiency or a low cost. [11]

2.3.2 Wind turbine

Wind turbine's working principle is the opposite of a fan. Instead of using electricity to make wind like a fan, wind turbines use wind to generate electricity. When the wind blows, the combination of lift and drag forces on turbine blades causes the rotor to spin, and the turning shaft spins a generator to generate electricity. In general, the gear box is used to connect the rotor and generator which turns the slow rotation of the blades into a quicker

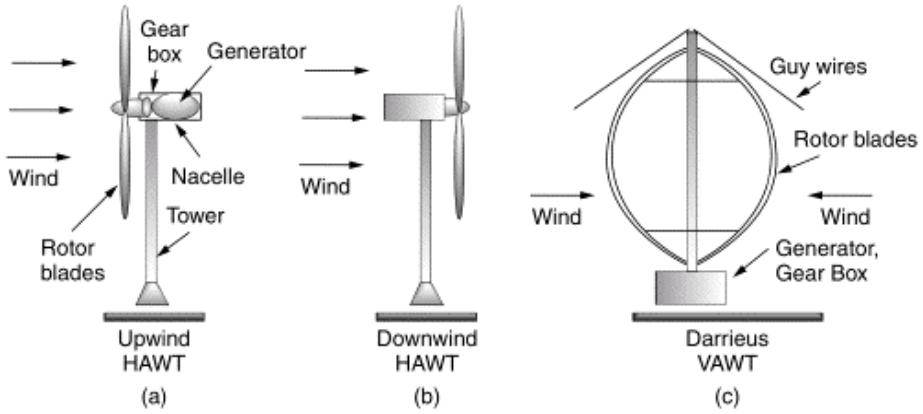

Figure 2.2: Horizontal axis wind turbines (HAWT) are either upwind machines (a) or down wind machines (b). Vertical axis wind turbines (VAWT) accept wind from any direction [13]

rotation that is more suitable for electricity generation. [12]

Wind turbines can be separated into two types based on the axis about which the turbine rotates. Most are horizontal axis wind turbines (HAWT), but there are some with blades that spin around a vertical axis (VAWT). Different types of wind turbines are shown in Fig 2.2. Wind turbines can also be classified by the location in which they are to be used: onshore, nearshore or offshore. [13] The wind turbines can classified by the size: small scale is defined as wind generation systems with capacities of 10 kW or less and are usually used to power homes, farms, and small businesses, middle scale is defined as wind generation systems with capacities from 10 kW to 100 kW and large scale is defined as wind generation systems with capacities larger than 100 kW.

2.3.3 Balance of the system

"Balance of the system" or BOS refers to the system components between the generator and the load that enables the electricity generated by the renewable generator to be properly applied to the load. The BOS frequently account for half of the system cost and most of the system maintenance.

Inverter

An inverter is a circuit for converting direct current (DC) to alternating current (AC), which acts as the interface between the PV arrays and the utility grid in a grid connected HPWS.

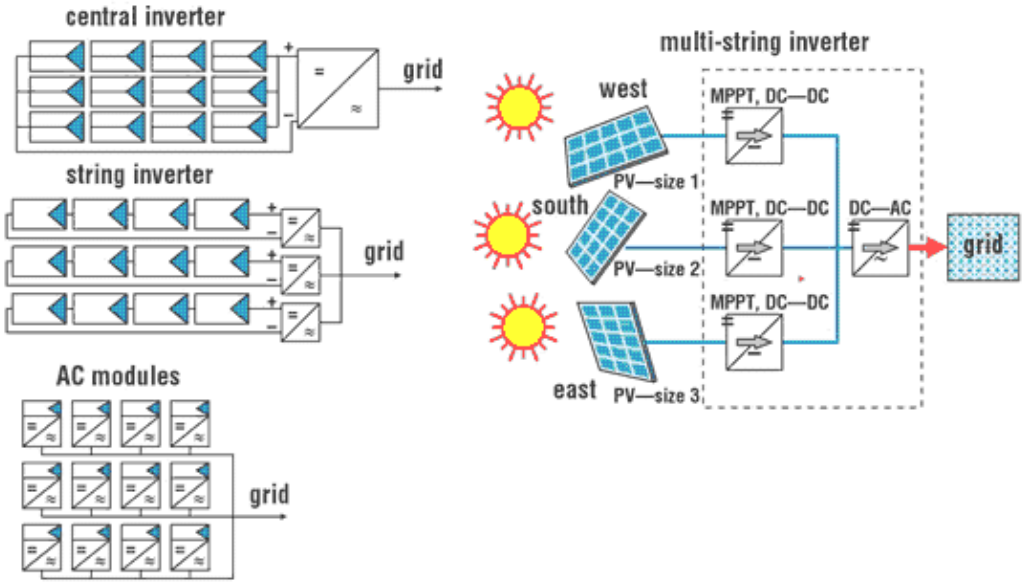

Figure 2.3: Basic design concepts for PV installations: central, string, multi-string or AC module inverters [14]

The inverter can perform a wide variety of functions: The basic function is to change low voltage DC power which is produced by the PV arrays into standard AC with high conversion efficiency and a suitable quality. Maximum Power Point Tracking (MPPT) is another main function; the inverter system uses a control algorithm to keep the PV arrays performing close to their peak power point when the solar radiation varies. The inverter also has protective function to operate in disconnection and isolation when faults or interrupting occurs in either side of the hybrid system. Inverter generally offers monitoring and reporting of the various parameters to the remote computer terminal or data logger. [15]

Over the last decade, photovoltaic inverter technology has evolved rapidly following the boom of the PV market. New inverter designs have been developed for the market (Fig 2.3). In general, the inverters can be classified as [14]:

- Central inverters
- String inverters
- Module integrated inverters (AC modules)
- Multi-string inverters

PV modules mounting and wind turbine tower

PV modules mounting and wind turbine tower are engineered to withstand the PV modules and the wind turbine. The PV modules mounting can be a ground mount that works either on rooftops or the ground, or pole mount for getting them up in the air. Both are angle-adjustable so that PV array will face the sun as near to perpendicular as possible. PV mounting racks can be adjusted two to four times a year to get maximum exposure as the sun changes its angle during seasons. Or if the rooftop has a good angle to the sun, the modules could be mounted solidly to the roof without an adjustable rack. Trackers are another PV mounting option, which are pole mounts that automatically adjust themselves so that the PV could face the sun throughout the day. Because the wind turbine should be mounded into non-turbulent wind, a tall enough wind turbine tower is needed. And there should also be enough space to properly anchor the guy wires.

Monitoring and instrumentation

Meters and instruments are important components in HPWS for acquiring meteorological data, monitoring and collecting system output data. In this research, these needed to be weather- and UV-resistant and also specified for low temperature usage. Monitoring HPWS permits examination of its behavior under real operating conditions. Instruments and connecting cables, more or less suitable for cold climate measurements, are continuously being developed and evaluated by manufacturers and users [16].

Commercial weather station containing different sensors and meters are available to offer accurate meteorological data. Solar irradiance, wind speed, wind direction, PV in-plane and ambient temperature, pressure and humidity are the most commonly monitored meteorological parameters. There are three main types of sensors that measure solar irradiance: thermopile pyranometers, reference cells, and photodiodes. Anemometer and vane are widely used to measure wind speed and direction. [17]

For analytical system monitoring it is common to sample instantaneous quantities like voltage, current, power, and energy output at regular intervals, and then those sampled values are averaged in order to limit the amount of data to be stored and processed. [17]

Safety equipment

Safety equipment includes over-current and lightning protection components. Over-current protection components such as fuses and fused disconnects protect the system's wiring and components in the event of short circuits. Fusing

protects from over-current situations, and disconnects allow safe shutdown of system components for maintenance and repair. Fuses and fused disconnects are rated by the amount of current they can handle. They may be as small as a few amperes for supplying metering to as large as 400 amperes for supplying the inverter. Many renewable energy systems are in areas where thunderstorms and lightning are common, especially, the wind turbine is always the highest structure in the remote area. Commercial lightning arrestors are available to help protect RE system electronics against the lightning.

2.4 The effect of cold climate on HPWS

2.4.1 The effects on photovoltaic

Photovoltaic cells perform slightly differently in cold climates than the normal ones. In Ref [18], a number of effects on photovoltaic were summerized. Cold cell temperatures, low light levels, altered light spectrum, high incidence angles of the sun's rays and snow and ice accumulation all affect the cell's operational characteristics.

It has been widely noticed that at the same solar insolation condition, as PV cell temperature increases, the power output decreases substantially; most PV cells work better in cold clear days than in hot ones [19]. A peak power and open-circuit voltage of most types of modules tends to improve by about 0.3 % to 0.5 % for every degree Celsius drop in the cell temperature.

In many cold climate regions, days are longer and a lot of energy is available in summer, while winter is darker and cloudier than other seasons. As a result the seasonal variation in the solar resource is much more pronounced than at more equatorial locations. Most PV modules are less efficient under weak lighting.

During winter at moderate and high latitudes, the sun is low in the sky and its light must pass through more air. This tends to scatter the blue light and the sun's rays become relatively redder as a consequence, this has little effect on some types of PV cells, *e.g.*, crystalline silicon cells.

In cold climates region, snow and ice accumulate on the array, blocking the sunlight, and reducing the electrical output. Snow and ice accumulation can cause a loss of 1.4 % to 3.5 % of the annual energy production [18]. The effect can be minimized by number of ways, such as higher tilt angles, mounting rectangular modules, manual removal of snow and ice, passive melting technologies and so on.

2.4.2 The effects on wind turbine

Wind turbines in cold climates refer to sites that have either icing events or low temperatures (lower than $-20\,^{\circ}\mathrm{C}$) outside the operational limits of standard wind turbines. The cold climates effect on wind turbine are reported in IEA publications Refs. [20] and [21]:

The performance of an iced-up wind turbine will normally degrade rapidly as the ice accumulates. If the icing continues without proper anti-icing method, the turbine will either stop because of excess vibrations or disconnect from the grid because of increased aerodynamic drag that slows the rotor down. Blade heating system may be necessary or profitable at sites that experience frequent icing or have high safety requirements such as proximity to roads.

Based on the equation of state for an ideal gas, air at $30\,^{\circ}\mathrm{C}$ is $26.7\,\%$ denser than at $35\,^{\circ}\mathrm{C}$. Since power is proportional to air density, power output increases at lower temperatures. However, the qualities of steel and welding usually determine the lowest operational temperature limit for the turbine.

2.5 Design, installation and operation

The ultimate goal of the design, installation and operation of a HPWS should be to maximize the energy production, minimize the life-cycle cost of the system while satisfying constraints on reliability, availability of capital, operational and maintenance requirements and environmental impact. [8]

Best practice guidelines and instruction for implementing PV and wind energy system are available from many national, international, professional, and industrial organizations. These should be used as often as possible, even though they do not generally consider cold climates. Examples of the guidelines include:

- IEC 60364-7-712, Electrical installations of buildings - Part 7-712: Requirements for special installations or locations - Solar photovoltaic (PV) power supply systems [22]
- DTI/Pub URN 02/788, Photovoltaics in Buildings - Guide to the installation of PV system [23]
- Wind resource assessment handbook [24]
- IEC 61400-2, Safety Requirements for Small Wind Turbines [25]
- IEA Wind Task II Recommended Practices. [26]

Specific issues such as accessibility, temperature, ice, snow, energy potential, technology, economic risk, public safety, infrastructure, and labor safety will require additional thought. [21]

2.6 Performance Analysis

2.6.1 Photovoltaic system analysis

The PV system performance is analysed following two monitoring procedures given in:

1. IEC 61724 Photovoltaic system performance monitoring-guidelines for measurements, data exchange and analysis. [5]

2. EUR 16339EN Guidelines for the assessment of photovoltaic plants document B: analysis and presentation of monitoring data. [27]

The irradiance is usually used to describe the solar energy availability. Irradiance is the rate at which radiant energy is incident on a surface in W/m^2. Irradiation is the incident energy per unit area, found by integration of irradiance over a specified time period. Insolation is a term applied specifically to solar energy irradiation and the unit of insolation is kWh/m^2. [28]

In this research, the symbol H and I are used for daily and hourly insolation, respectively. Symbol G is used for solar irradiance. Subscripts of G, H and I are as follows:

- g and T refer to radiation on a horizontal and tilted plane, respectively.

- b, d and r refer to beam, diffuse and reflected radiation, respectively.

Subscripts of system parameters are as follows:

- a and s (or f) refer to parameters for array and system, respectively.

- d and m refer to daily and monthly parameters, respectively.

- (1) and (2) refer to parameters for PV array-1 and PV array-2, respectively.

- inv refers to parameters for inverters.

Solar insolation on tilted PV array

The first move for analyzing the performance of a tilted PV array is to determine the solar radiation. In some cases, the horizontal solar irradiance or insolation are the only data that can be acquired during the monitoring period, therefore, we need to convert solar irradiance or insolation on horizontal surface to the values on tilted surface. M. Kolhe *et al.* described a conversion method in Ref. [29]:

The daily tilted insolation (H_T) can be expressed as:

$$H_T = H_g R_{bd} - H_d R_{bd} + H_d R_d + R_r H_g, \tag{2.1}$$

where R_{bd} is the tilt factor for the daily direct solar insolation, which is defined as:

$$R_{bd} = \frac{\omega_{st} \sin\delta \sin(\phi - \beta) + \cos\delta \sin\omega_{st} \cos(\phi - \beta)}{\omega_s \sin\delta \sin\phi + \cos\phi \cos\delta \sin\omega_{st}}, \tag{2.2}$$

where ω_s and ω_{st} are sunrise and sunset hour angles on a horizontal PV array, respectively, and are defined as:

$$\omega_s = \cos^{-1}(-\tan\phi \tan\delta) \tag{2.3}$$

and

$$\omega_{st} = \cos^{-1}[-\tan(\phi - \beta)\tan\delta], \tag{2.4}$$

where ϕ, δ and β are location latitude, declination angle, and PV module tilted angle, respectively. The declination angle δ (in rad) is defined as:

$$\delta = \frac{\pi}{180} 23.45 \sin\left[\frac{2\pi}{365}(284 + j_d)\right], \tag{2.5}$$

where j_d is the number of the day in a year.

The tilt factors R_d and R_r for the diffuse and reflected part of the solar radiation, respectively, are defined as:

$$R_d = \frac{1 + \cos\beta}{2} \tag{2.6}$$

and

$$R_r = \rho \frac{1 - \cos\beta}{2}, \tag{2.7}$$

where ρ is ground reflectivity. The average value of ground reflectivity is 0.36.

Studies of available daily radiation data have shown that the average fraction of the diffuse radiation component H_d/H_g is a function of K_T, the

day's clearness index. Equation representing the correlation by Collares-Pereira and Rabl (1979) is used in this research [30]:

$$H_d/H_g = \begin{cases} 0.99 & \text{for } K_T \leq 0.17 \\ 1.188 - 2.272K_T + \\ \ 9.473K_T^2 - 21.865K_T^3 + \\ \ 14.648K_T^4 & \text{for } 0.17 < K_T < 0.75 \\ -0.54K_T + 0.632 & \text{for } 0.75 \leq K_T < 0.80 \\ 0.2 & \text{for } K_T \geq 0.80 \end{cases} \tag{2.8}$$

where the clearness index K_T is defined as:

$$K_T = H_g/H_o, \tag{2.9}$$

where H_o (unit: $\mathrm{Wh/m^2}$) is the daily solar insolation on an extra-terrestrial flat surface and is given by:

$$H_o = \frac{24}{\pi} G_{st} \left[1 + 0.033\cos(\frac{2\pi j_d}{365})\right](\cos\phi\cos\delta\sin\omega_s + \omega_s\sin\phi\sin\delta), \tag{2.10}$$

where solar constant $G_{st} = 1367\mathrm{W/m^2}$.

Daily and monthly array and system yields

The normalized power values, averaged over a period of the PV plant operation, are called "yields". The yield can also be considered as the number of hours of array or system operation per day at PV rated power. The reference yield is the yield of an ideal array with the same spectral response as the reference cell and without any temperature effects on power. It is defined as the theoretically available energy per day per 1 $\mathrm{kW_p}$, given by:

$$Y_{r,d} = \frac{H_{T,d}}{G_{STC}}, \tag{2.11}$$

where G_{STC} is the solar irradiance under Standard Test Condition (STC), which means the air mass is 1.5, the solar irradiance value is $G_{STC} = 1000\ \mathrm{W/m^2}$ and the cell temperature is 25 °C. [31]

The daily array yield ($Y_{a,d}$) and the system final yield ($Y_{f,d}$) are defined as:

$$Y_{a,d} = \frac{E_{a,d}}{P_{PV,rated}} \tag{2.12}$$

and

$$Y_{f,d} = \frac{E_{s,d}}{P_{PV,rated}}, \tag{2.13}$$

where $E_{a,d}$ is the total daily energy output from PV array, and $E_{s,d}$ is the total daily energy output from the PV system. The unit of yield is h/d.

The monthly average daily array yield ($Y_{a,m}$) and monthly average daily final yield ($Y_{f,m}$) are defined as:

$$Y_{a,m} = \frac{1}{N} \sum_{d=1}^{N} Y_{a,d} \tag{2.14}$$

and

$$Y_{f,m} = \frac{1}{N} \sum_{d=1}^{N} Y_{f,d}, \tag{2.15}$$

where N is the number of days in a month.

Capture and system losses

The normalized losses of the system can be defined as the differences between the yields, *i.e.*, capture losses by

$$L_c = Y_r - Y_a \tag{2.16}$$

and system losses by

$$L_s = Y_a - Y_f. \tag{2.17}$$

Daily and monthly PV array and system efficiencies

Daily PV array and system efficiencies are defined as:

$$\eta_{a,d} = \left(\frac{E_{a,d}}{H_{T,d} * A} \right) \times 100\% \tag{2.18}$$

and

$$\eta_{s,d} = \left(\frac{E_{s,d}}{H_{T,d} * A} \right) \times 100\%, \tag{2.19}$$

where A is the total area of PV array, $E_{a,d}$ is the energy output from PV array and $E_{s,d}$ is the energy output from PV system.

The monthly PV array and system efficiencies are calculated using two methods. In *the first method*, the daily PV array and system efficiencies are averaged over a month as:

$$\bar{\eta}_{a,m} = \left(\frac{1}{N} \sum_{d=1}^{N} \eta_{a,d} \right) \times 100\% \tag{2.20}$$

and

$$\bar{\eta}_{s,m} = \left(\frac{1}{N} \sum_{d=1}^{N} \eta_{s,d} \right) \times 100\%. \tag{2.21}$$

In *the second method*, the monthly total array and system outputs and monthly total in plane insolation are used to calculate the monthly PV array efficiency ($\eta_{a,m}$) and system efficiency ($\eta_{s,m}$) are as:

$$\eta_{a,m} = \left(\frac{\sum_{d=1}^{N} E_{a,d}}{\sum_{d=1}^{N} H_{T,d} \times A} \right) \times 100\% \tag{2.22}$$

and

$$\eta_{s,m} = \left(\frac{\sum_{d=1}^{N} E_{s,d}}{\sum_{d=1}^{N} H_{T,d} \times A} \right) \times 100\%. \tag{2.23}$$

Daily and monthly inverter performances

The daily inverter efficiency is calculated from the daily total PV array and system outputs:

$$\eta_{inv,d} = \left(\frac{E_{a,d}}{E_{s,d}} \right) \times 100\%. \tag{2.24}$$

The monthly inverter efficiency is calculated as shown below:

$$\bar{\eta}_{inv,m} = \left(\frac{1}{N} \sum_{d=1}^{N} \eta_{inv,d} \right) \times 100\% \tag{2.25}$$

and

$$\eta_{inv,m} = \left(\frac{\sum_{d=1}^{N} E_{s,d}}{\sum_{d=1}^{N} E_{a,d}} \right) \times 100\%. \tag{2.26}$$

Daily and monthly performance ratios

The performance ratio (PR) is the rating most commonly used to describe the power conditioning of a grid-connected PV system [32]. The daily performance ratio is defined as the ratio of the daily final yield to the daily reference yield:

$$PR_{a,d} = \frac{Y_{a,d}}{Y_{r,d}} = \frac{Y_{a,d} G_{STC}}{H_{T,d}} \tag{2.27}$$

and

$$PR_{s,d} = \frac{Y_{f,d}}{Y_{r,d}} = \frac{Y_{f,d} G_{STC}}{H_{T,d}}, \tag{2.28}$$

where G_{STC} is the solar irradiance in Standard Test Condition.

The monthly average daily array and system performance ratio PR are given by

$$\overline{PR}_{a,m} = \frac{1}{N}\sum_{d=1}^{N} PR_{a,d} \tag{2.29}$$

and

$$\overline{PR}_{s,m} = \frac{1}{N}\sum_{d=1}^{N} PR_{s,d}. \tag{2.30}$$

The monthly array and system performance ratios are given by

$$PR_{a,m} = \left(\frac{\sum_{d=1}^{N} E_{a,d}}{\sum_{d=1}^{N} H_{T,d}}\right)\left(\frac{G_{STC}}{P_{PV,rated}}\right) \tag{2.31}$$

and

$$PR_{s,m} = \left(\frac{\sum_{d=1}^{N} E_{s,d}}{\sum_{d=1}^{N} H_{T,d}}\right)\left(\frac{G_{STC}}{P_{PV,rated}}\right). \tag{2.32}$$

2.6.2 Wind power system analysis

There are several probability density functions, also called continuous mathematical functions, that can be used to model the wind speed frequency curve by fitting time series measured data. In wind power studies, two parameter Weibull probability density function is commonly used and widely adopted [33]. Zero wind speed records are generally ignored in Weibull probability density functions, therefore, a Hybrid Weibull distribution including calm periods was introduced by E.S. Takle and J.M. Brown in 1977 [34]. Because of its higher accuracy, Hybrid Weibull distribution was used to analyze wind speed in this research.

Weibull distribution of wind speed

The Weibull probability density function is a special case of a generalized two parameter Gamma distribution. Weibull distribution can be characterized by its probability density function $f(V)$ and its cumulative distribution function $F(V)$ [33]:

$$f(V) = \frac{k}{c}\left(\frac{V}{c}\right)^{k-1} e^{-(V/c)^k} \tag{2.33}$$

and

$$F(V) = 1 - e^{-(V/c)^k}, \tag{2.34}$$

where k is the shape parameter, c is the scale parameter, V is wind speed. The scale and shape parameters can be estimated by using the maximum

likelihood method [35]:

$$k = \left(\frac{\sum_{i=1}^{n} V_i^k \ln(V_i)}{\sum_{i=1}^{n} V_i^k} - \frac{\sum_{i=1}^{n} \ln(V_i)}{n} \right)^{-1} \tag{2.35}$$

and

$$c = \Big(\frac{1}{n} \sum_{i=1}^{n} V_i^k \Big)^{1/k}, \tag{2.36}$$

where V_i is the wind speed at time step i and n is the number of non–zero wind speed data points.

The Hybrid Weibull distribution can be expressed as [34]:

$$f^H(V) = F_0 \delta(V_i) + (1 - F_0) f(V) \quad \text{for } V_i \geq 0, \tag{2.37}$$

where F_0 is the probability of observing zero wind speed and $\delta(V_i)$ is the Dirac delta function:

$$\delta(V_i) = \begin{cases} 0 & \text{for } V_i \neq 0 \\ 1 & \text{for } V_i = 0. \end{cases} \tag{2.38}$$

The Hybrid Cumulative Weibull distribution is given by:

$$F^H(V) = F_0 + (1 - F_0) F(V), \quad \text{for } V \geq 0. \tag{2.39}$$

As the scale and shape parameter have been calculated, two meaningful wind speeds—the most probable wind speed and the wind speed carrying maximum energy—can easily be obtained. The most probable wind speed denotes the most frequent wind speed for a given wind probability distribution and the wind speed carrying maximum energy represents the wind speed which carries the maximum amount of wind energy. They can be expressed as [33]:

$$V_{MP} = c \left(\frac{k-1}{k} \right)^{1/k} \tag{2.40}$$

and

$$V_{MaxE} = c \left(\frac{k+2}{k} \right)^{1/k}. \tag{2.41}$$

Moist air density

The wind power varies linearly with the air density sweeping the blades. The 1981 Equation for the density of moist air has the following form [36]:

$$\rho = \frac{p M_a}{Z R T} \left[1 - x_v (1 - \frac{M_V}{M_a}) \right], \tag{2.42}$$

Table 2.1: Constant parameters specified for the 1981 equation for the determination of the density of moist air [36]

Parameters	1981	1991
Vapor pressure at saturation p_{sv}		
$A/(10^{-5}\,\mathrm{K}^{-2})$	1.2811805	1.2378847
$B/(10^{-2}\,\mathrm{K}^{-1})$	-1.9509847	-1.9121316
C	34.04926034	33.93711047
$D/(10^{3}\,\mathrm{K})$	-6.3536311	-6.3431645
Enhancement factor f		
α	1.00062	1.00062
$\beta(10^{-8}\,\mathrm{Pa}^{-1})$	3.14	3.14
$\gamma(10^{-7}\,\mathrm{Pa}^{-2})$	5.6	5.6
Compressibility factor Z		
$a_0/(10^{-6}\,\mathrm{KPa}^{-1})$	1.62419	1.58123
$a_1/(10^{-8}\,\mathrm{Pa}^{-1})$	-2.8969	-2.9331
$a_2/(10^{-10}\,\mathrm{K}^{-1}\mathrm{Pa}^{-1})$	1.0880	1.1043
$b_0/(10^{-6}\,\mathrm{KPa}^{-1})$	5.757	5.707
$b_1/(10^{-8}\,\mathrm{Pa}^{-1})$	-2.589	-2.051
$c_0/(10^{-4}\,\mathrm{KPa}^{-1})$	1.9297	1.9898
$c_1/(10^{-6}\,\mathrm{Pa}^{-1})$	-2.285	-2.376
$d/(10^{-11}\,\mathrm{K}^{2}\mathrm{Pa}^{-2})$	1.73	1.83
$e/(10^{-8}\,\mathrm{K}^{2}\mathrm{Pa}^{-2})$	-1.034	-0.765
Gas constant R		
$R/(\mathrm{Jmol}^{-1}\mathrm{K}^{-1})$	8.31441	8.314510
Leading constant $M_a(x_{CO_2} = 0.0004)/R$, in equation for the density of moist air		
$M_a R^{-1}/(10^{-3}\,\mathrm{kgKJ}^{-1})$	3.48353	3.48349

where p is the pressure, T is the thermodynamic temperature, x_v is the mole fraction of water vapor, M_a is the molar mass of dry air, M_V is the molar mass of water, R is the molar gas constant, and Z is the compressibility factor.

The auxiliary equation for M_a is

$$M_a = [28.9635 + 12.011(x_{CO_2} - 0.0004)] \times 10^{-3}, \tag{2.43}$$

where the M_a unit is kg/mol, x_{CO_2} is the mole fraction of carbon dioxide.

The mole fraction of water vapor x_v is not measured directly. Instead, it is derived from a measurement of the relative humidity h. The saturation vapor pressure of moist air $p_{SV}(t)$ can be obtained from auxiliary equation:

$$p_{SV} = 1 \times \exp(AT^2 + BT + C + D/T), \tag{2.44}$$

where A, B, C and D are constant parameters.

Also the enhancement factor f is calculated from:

$$f = \alpha + \beta p + \gamma t^2, \tag{2.45}$$

where t is temperature in degrees Celsius.

Recall that

$$x_V = hf(p,t)\frac{p_{SV}(t)}{p}. \tag{2.46}$$

Finally, the compressibility Z is calculated from the equation:

$$Z = 1 - \frac{p}{T}[a_0 + a_1 t + a_2 t^2 + (b_0 + b_1 t)x_V + (c_0 + c_1 t)x_V^2] + \frac{p^2}{T^2}(d + e x_V^2). \tag{2.47}$$

Table 2.1 shows constant parameters specified for the 1981 equation for the determination of the density of moist air. The amended 1991 parameters are used in this research.

Wind power density

Wind power density of a site based on a Weibull probability density function can be expressed as [33]:

$$\frac{P}{A} = \int_0^\infty P(V) f(V) dV = \frac{1}{2}\rho c^3 \Gamma\left(\frac{k+3}{k}\right), \tag{2.48}$$

where A is turbine blade swept area, ρ is the moist air density, Γ denotes the Gamma function.

Wind energy generated by an ideal wind turbine

For a ideal wind turbine, the wind energy available in the wind can be completely extracted, the energy generated by an ideal wind turbine can be expressed as:

$$\begin{aligned} E_{TW} &= \frac{\rho}{2}TA\int_{V_I}^{V_R} V^3 \frac{k}{c}(\frac{V}{c})^{k-1}e^{-(\frac{V}{c})^k}dV \\ &\quad +\frac{\rho}{2}TAV^3\int_{V_R}^{V_O} \frac{k}{c}(\frac{V}{c})^{k-1}e^{-(\frac{V}{c})^k}dV, \end{aligned} \tag{2.49}$$

where V_I, V_R, and V_O are cut-in, rated, and cut-out speed of the ideal wind turbine, respectively. The integrals cannot be analytically solved, but they can be easily calculated by any typical numerical integration techniques such as Simpson's rule or Gauss quadrature. Herein the Simpson's rule was used.

Actual wind energy output from a wind turbine

The wind energy available in the wind cannot be extracted completely by any real wind turbine, as the air mass would be stopped completely in the intercepting rotor area. The actual wind power output from the wind turbine is determined by the turbine performance curve given by:

$$P_T(V) = \begin{cases} 0 & \text{for } V < V_I \\ (a_1V^4 + a_2V^3 + a_3V^2 + a_4V + a_5)P_R & \text{for } V_I \le V < V_R \\ P_R & \text{for } V_R \le V < V_O \\ 0 & \text{for } V \ge V_O \end{cases} \tag{2.50}$$

where a_1, a_2, a_3, and a_4 are regression constants of the turbine performance curve. The regression constants were measured from the wind speed—power curve that is offered by the manufacturer (directly from power curve. See Fig. 2.4). For WT-10P wind turbine: a_1=-0.00041, a_2=0.01221, a_3=-0.11726, a_4=0.51973, a_5=-0.84333.

The actual wind energy out put from a wind turbine is given by:

$$\begin{aligned} E_{TA} &= T\int_{V_I}^{V_O} P_T(V)f(V)dV \\ &= TP_R\int_{V_I}^{V_R} \left(a_1V^4 + a_2V^3 + a_3V^2 + a_4V + a_5\right)\frac{k}{c}\left(\frac{V}{c}\right)^{k-1} e^{-\left(\frac{V}{c}\right)^k}dV \\ &\quad +TP_R\int_{V_R}^{V_O} \frac{k}{c}\left(\frac{V}{c}\right)^{k-1} e^{-\left(\frac{V}{c}\right)^k}dV, \end{aligned} \tag{2.51}$$

where T is the mornitoring period (or duration).

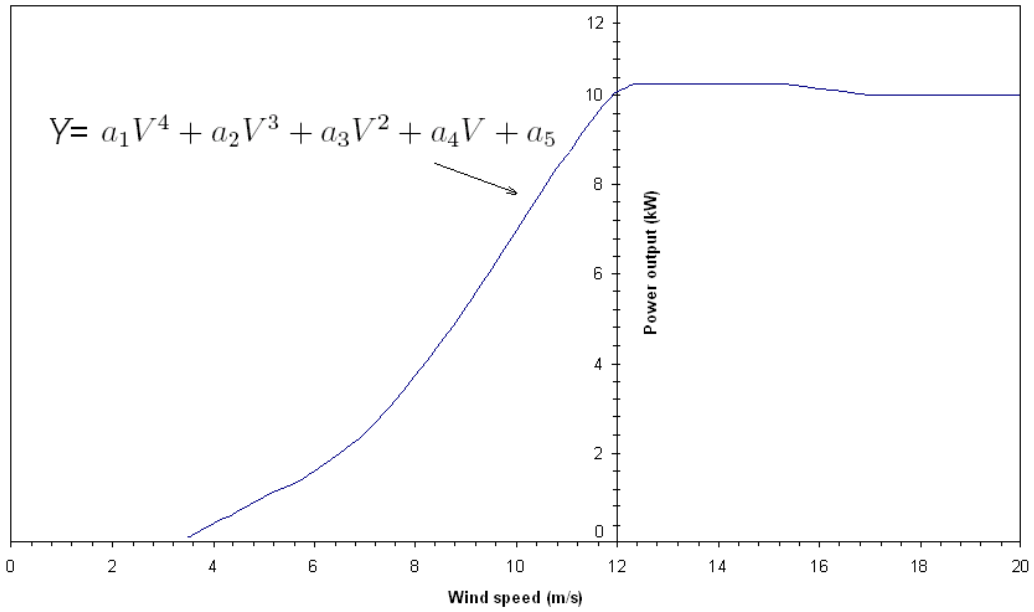

Figure 2.4: WT 10P wind speed—power curve

Wind turbine efficiency, capacity factor, and wind availability factor

The wind turbine efficiency is defined as the ratio of the actual wind energy output from a wind turbine to the wind energy generated by an ideal wind turbine:

$$\eta = \frac{E_{TA}}{E_{TW}}. \tag{2.52}$$

According to Betz law, the theoretically maximum power that can be extracted from the wind is 59% of the wind power available in the wind. Therefore, for any wind turbine, the efficiency should not exceed 0.59.

The capacity factor is another important index in measuring the productivity of a wind turbine. It is defined as:

$$C_F = \frac{E_{TA}}{TP_R}, \tag{2.53}$$

where T is the time period (or duration).

The wind availability factor is of the time percentage of wind speed between turbine cut-in and cut-off speed. It is defined as:

$$A_F = \frac{T_i}{T_T}, \tag{2.54}$$

where T_i is the number of hours that wind speed is between turbine's cut-in and cut-off speed. T_T is the total hours in monitoring period.

Site turbulence intensity

The turbulence intensity is a site characteristic, because high turbulence levels may decrease power output and cause extreme loading on wind turbine components. It is defined as

$$TI = \frac{\sigma}{V}, \tag{2.55}$$

where σ is standard deviation in 10 min wind speed, and V is 10 min average wind speed.

The data recovery rate

The data recovery rate is defined as the number of valid data records collected versus that possible over the reporting period.

Chapter 3

System Description

In this chapter, the Hybrid Photovoltaic (PV) and Wind Electricity Generation System (HPWS) in Viitasaari ABC service station consisting of a PV sub-system, a wind electricity sub-system, and the monitoring system is described.

Figure 3.1: ABC service station in the city of Viitasaari

3.1 Location

The ABC service station (latitude: $63°4'27''N$, and longitude: $25\ °52'7''E$) owned by Keskimaa Co-operative is situated in the southeast corner of the city of Viitasaari located in Central Finland. The service station has a 24-hour operated petrol filling station, a restaurant and a convenient store. The electricity demand of the station is partly supplied by a 4.16 kW_p PV system and a 10 kW wind turbine. Fig. 3.1 shows the ABC service station in Viitasaari.

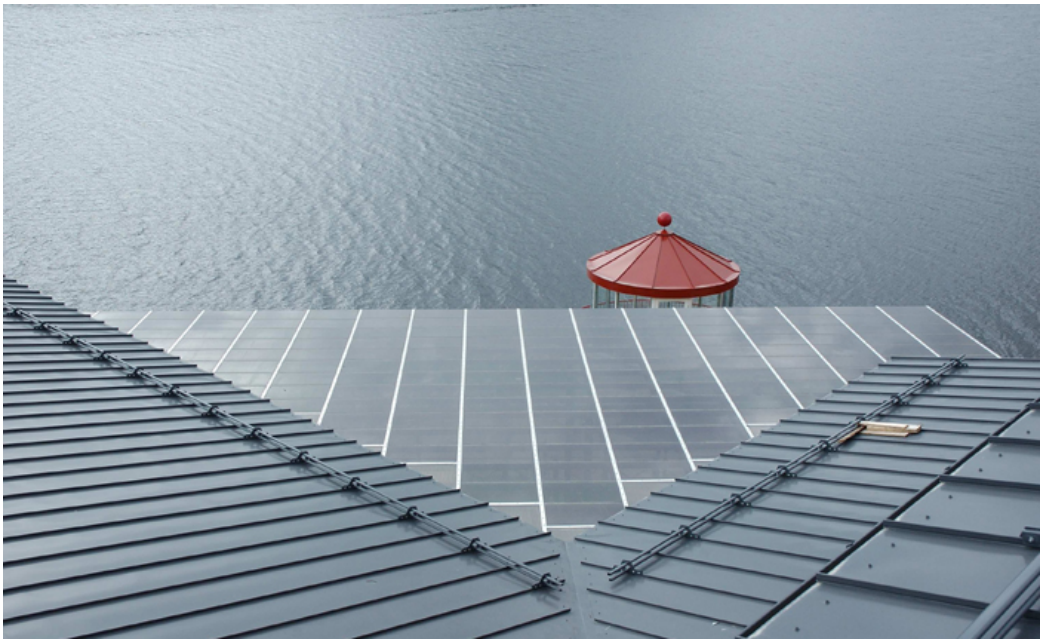

Figure 3.2: The PV arrays at ABC service station

3.2 PV sub-system

The PV sub-system consisted of two PV arrays (PV array-1 and PV array-2, see Appendix A) that produce electricity directly from solar radiation. The direct current (DC) outcoming from the arrays was converted to alternating current (AC) by two inverter units, respectively, and fed into station's grid through the switchboard. The semi-transparent solar arrays were also functioning as a canopy of the station's terrace. The Fronius IG DatCom system is used for monitoring the PV sub-system. The PV array at the station is shown in Fig 3.2.

The installed PV arrays are facing south inclined 5° from the horizontal. They contained 154 thin-film SCHOTT ASITHRU-30-SG PV modules, that are made of a glass front pane with amorphous silicon ASI tandem cells, PVB foil and a heat strengthened backing glass [37]. Both PV arrays contained eleven strings of seven modules that are connected in series. The arrays were connected to Fronius IG 60 inverters through a junction box. The inverters were connected to the station's switchboard to feed electricity to the building's grid. The Fronius IG inverters were equipped with High Frequency (HF)-transformer, Maximum power point (MPP) tracking, automatic switching on-off, grid monitoring, fault identification and basic recording function [38]. Tables 3.1, 3.2 and 3.3 summarize the characteristic parameters of the PV module, array and inverter, respectively.

Table 3.1: PV module characteristic parameters [37]

Parameter	PV Module
Maxiumum power	27 W_p
Max. power voltage	36 V
Max. power current	0.75 A
Open circuit voltage	49 V
Short circuit current	1.02 A
Area	0.6 m^2
Weight	14 kg

Table 3.2: PV arrays characteristic parameters

Parameter	PV Array
Maxiumum power	2.08 kW_p
Number of strings	11
Number of modules in each string	7
Total number of modules in array	77
Total Area	46.2 m^2
Array voltage at max. power	252 V
Array current at max. power	8.25 A
Array open circuit voltage	343 V
Array short circuit current	11.22 A

Table 3.3: Inverters characteristic parameters [38]

Parameter	Inverter IG 60
MPP voltage range	$150 - 400$ V
Max. input voltage (at 1 kW/m^2; -10°C)	500 V
PV array power output	$4.6 - 6.7$ kW$_p$
Nominal power output	4.6 kW
Max. power output	5 kW
Max. efficiency	94.5 %
Euro efficiency	93.5 %
Mains voltage/frequency	230 V/50 Hz

3.3 Wind electricity sub-system

The 10 kW 3-blade horizontal axis wind turbine WT-10P manufactured by Windtower Deutschland was mounted on a 30 m high billboard tower of the service station where the distance from hub to the ground was 35 m. Fig. 3.3 shows the wind turbine WT-10P. The rotor was driving a asynchronous generator by a planetary gear box. The WT-10P was equipped with a microprocessor based control and protection system, the rotor was pitch controlled, yawing control was applied by a wind vane, and one electromagnetic brake was used to protect the generator. Table 3.4 summarizes the characteristic parameters of the WT-10P wind turbine.[39]

Table 3.4: WT 10P wind turbine characteristic parameters

Parameter	WT 10P wind turbine
Rated power	10 kW
Rated wind speed	12 m/s
Cut-in wind speed	3.5 m/s
Cut-out wind speed	20 m/s
Survival wind speed	50 m/s
Rotor diameter	5.4 m
Rotor swept area	22.9 m
Number of blades	3
Generator type	Asynchronous
Generator speed	1000 r/min
Generator voltage	400 V
Generator frequency	50 Hz
Nacelle weight	358 kg

The wind turbine was connected to the building's grid through a control

Figure 3.3: Wind turbine WT-10P in Viitasaari ABC servive station

electronic box, which was supplied by the manufacturer. Appendix B and C show the connection box and the schematic diagram of wind turbine system connection. There was one energy meter to measure the energy output of the WT-10P, however, the wind energy production values were not real time measured, only the accumulative values were casually recorded at the end of each month. Both the control electronic box and the energy meter were located inside the billboard tower.

3.4 Monitoring parameters

The monitoring system contains a Davis weather station, Fronius IG DatCom monitoring system, and RE-information center. The monitoring system was used to record meteorological and system output data and to monitor and display the system performance.

The Davis Cabled Vantage Pro2 $Plus^{TM}$ weather station was used for monitoring the meteorological data in this research. The weather station included two components: the Integrated Sensor Suite (ISS) and the console.

The ISS contained the sensor interface module, rain collector, anemometer , and a solar radiation sensor. Table 3.5 summarizes the weather data specifications. The console and ISS were powered by an AC-power adapter connected to the console that also used batteries as a backup power supply. WeatherLink was used for Vantage Pro2 $Plus^{TM}$ to interface with a computer, to log data and to upload weather information to the database. The ISS was arranged at the top of billboard tower on the tip of a porrect beam, which was approximate 30 m high from the ground. It is clearly seen in Fig. 3.3. The console was located inside the station. [40]

Table 3.5: Weather data specification [41]

Variable	Required sensors	Resolution	Range	Nominal accuracy
Barometric pressure	Included in console	0.1 hPa	880 to 1080 hPa	1.0 hPa
Outside Humidity	ISS or Tem/Hum Station	1%	0 to 100%	3% RH; 4% above 90%
Solar Radiation	Solar sensor	1 W/m^2	0 to 1800 W/m^2	5% of full scale
Outside Temperature	ISS or Tem/Hum Station	0.1 °C	−40 to +65 °C	0.5 °C
Time	Included in Console	1 min	24 h	8 s/month
Date	Included in Console	1 d	month/day	8 s/month
Wind Direction	Wind Vane	1 °	0 to 360 °	7 °
Wind Speed (small cups)	Anemometer	0.5 m/s	1.5 to 79 m/s	greater of 1 m/s or 5%

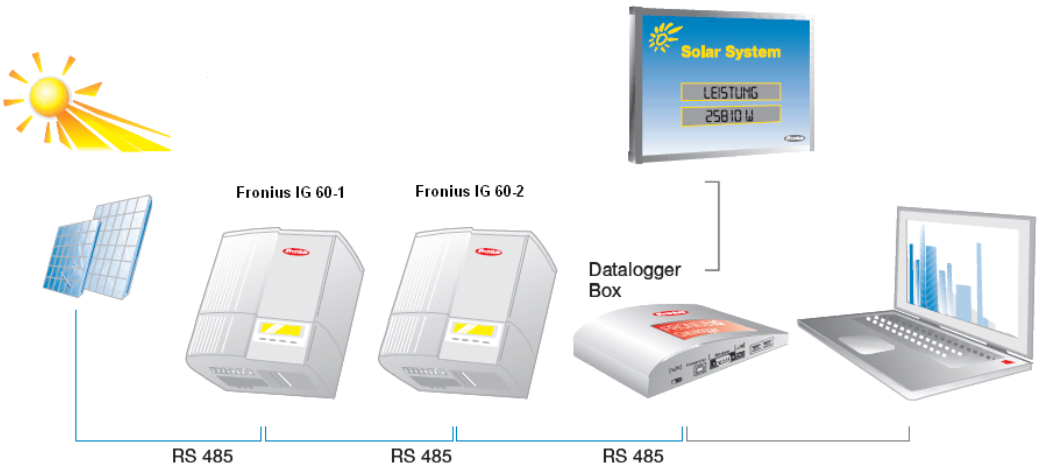

Figure 3.4: Fronius IG DatCom monitoring system connection scheme

The Fronius IG DatCom monitoring system was used for monitoring and recording PV sub-system data. It comprises network card, datalogger device, and data processing software. One COM card in each inverter was

operating as a network communication tool and the data from two inverters was recorded into a datalogger. The data was uploading from datalogger to computer with a 9-pin data cable. Data visualization, system administration and further processing functions were provided by Fronius *IG.access* software. The datalogger was connected to the inverter-1. Fig. 3.4 shows an example of connection scheme for the Fronius IG DatCom monitoring system. [42]

The RE-information center was situated next to the entrance of the building, it consisted of two display screens and two computers. Multimedia presentation of RE technology was shown on one screen, the slide show of heat and power production figures on the other screen.

The summary of the monitored parameters is shown in Table 3.6. The

Table 3.6: Monitored parameters

Parameter	Symbols	Unit
Wind speed	V	m/s
Wind direction	WD	°
Outside humidity	Hu	%
Pressure	P	bar
Solar insolation on horizontal surface	I_H	langley*
Ambient temperature	T_{amb}	°C
DC voltage from PV Array-1	$U_{a,1}$	V
DC current from PV Array-1	$I_{a,1}$	A
DC voltage from PV Array-2	$U_{a,2}$	V
DC current from PV Array-2	$I_{a,2}$	A
AC voltage from Inverter-1	$U_{s,1}$	V
AC current from Inverter-1	$I_{s,1}$	A
AC power from Inverter-1	$P_{s,1}$	W
AC voltage from Inverter-2	$U_{s,2}$	V
AC current from Inverter-2	$I_{s,2}$	A
AC power from Inverter-2	$P_{s,2}$	W
Energy supply to utility grid from Inverter-1	$E_{s,1}$	Wh
Energy supply to utility grid from Inverter-2	$E_{s,2}$	Wh
Energy supply to utility grid from wind turbine	E_w	Wh

* 1 langley=0.0116222 $\mathrm{kWh/m^2}$

wind turbine was connected to grid on 17 December 2004, and the data collecting from PV sub-system was started on 10 February 2005. The monitored period of this research started on 1 January 2005 and ended on 31 December 2006. The meteorological data from Davis was first set to record at 10 min

interval and then switched to 1 min interval on 7 April 2005. The data from Fronius IG monitoring system was first set to record at 15 min interval and then switched to 5 min on 7 April 2005.

Chapter 4

Analysis Results and Discussion

4.1 PV sub-system

The analysis started with data mining process, the meteorological data for the wind energy sub-system was based on the 10 min average value and the data for PV sub-system was based on the daily value. A statistical analysis software called R-Project[1] was used to analyze the HPWS performance. Over 689 days monitoring period, a total of 594 days records were examined in PV sub-system analysis. The missing records were due to either solar sensor or Fronius IG DatCom monitoring system malfunctions.

4.1.1 Solar insolation and ambient temperature

The solar insolation values over a day from the database were processed to obtain daily solar insolation on the horizontal surface ($H_{g,d}$). Then this value was converted to solar insolation on a 5° tilted surface ($H_{T,d}$) according to the formulations we described in Sec. 2.6.1. Table 4.1 shows the monthly total solar insolation on horizontal and on tilted surfaces and the monthly average ambient temperature over the monitoring period. These results show that the in-plane solar insolation is similar with the values of other PV system locations in Central or Western European countries during summer time [32, 43, 44]. We notice that the monthly average ambient temperature values in Central Finland region are much lower than in the other locations mentioned above. This indicates a weather condition that offers a better working environment for the PV cells.

Fig. 4.1 shows the daily in-plane solar insolation ($\bar{H}_{T,d}$) together with

[1]More information about R-Project can be found: http://www.r-project.org/

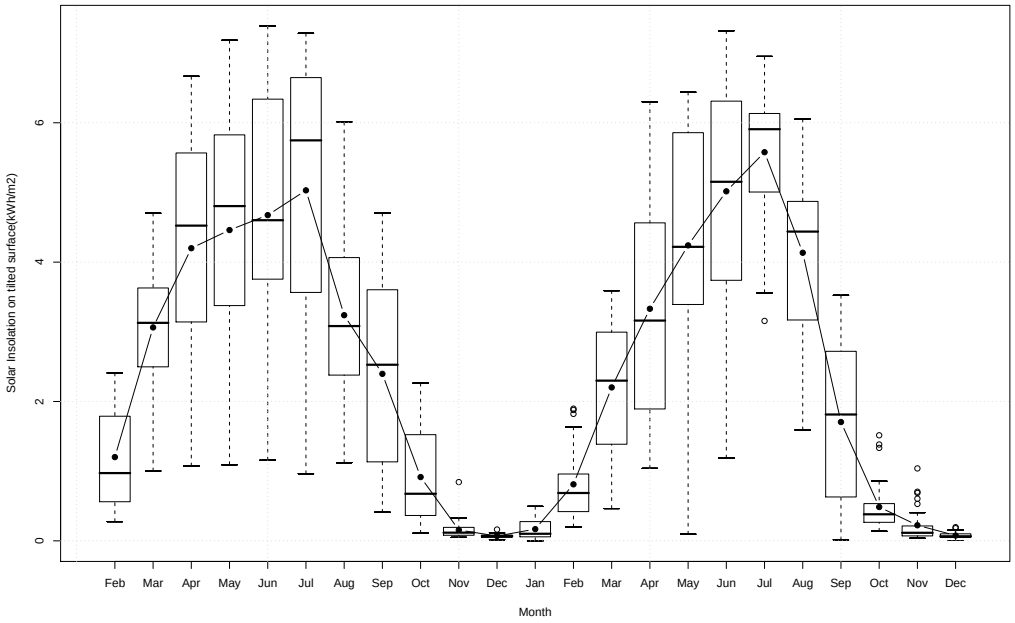

Figure 4.1: Monthly average of the daily in-plane solar insolation together with statistical box plot daily solar insolation over the monitored period

Table 4.1: Monthly total solar insolation on horizontal (H_g) and tilted (H_T) surface and averaged ambient temperature (T_{amb})

Month	2005			2006		
	H_g (kWh/m^2)	H_T (kWh/m^2)	T_{amb} (°C)	H_g (kWh/m^2)	H_T (kWh/m^2)	T_{amb} (°C)
Jan.	-	-	-	3.04	3.21	-9.34
Feb.	19.69	22.84	-9.31	20.26	22.71	-11.58
Mar.	84.09	94.95	-7.31	62.36	68.26	-6.58
Apr.	121.58	126.00	3.69	97.79	99.92	3.19
May	139.57	138.27	8.61	127.41	127.22	9.72
Jun.	143.80	140.24	14.11	154.48	150.49	15.61
Jul.	159.55	155.94	18.59	176.28	172.91	17.60
Aug.	99.00	100.40	15.54	126.44	128.18	18.18
Sep.	68.04	71.90	11.00	42.62	44.34	11.97
Oct.	26.03	28.37	5.78	14.25	15.05	4.61
Nov.	4.52	4.67	3.06	6.22	6.71	-0.56
Dec.	2.18	2.13	-6.23	2.57	2.37	1.21

the statistical boxplot[2] of the daily solar insolation on a monthly basis over the monitored period. The highest value of $\bar{H}_{T,d}$ was in July 2006 with 5.58 kWh/m^2, while the lowest value was in December 2005 with 0.07 kWh/m^2. We noticed that the solar energy resources were abundant in summer. However, the average daily solar insolation on the tilted surface were less than 2 kWh/m^2 in 83.3% of year, that means quite a small amount of electricity that can be generated using the PV arrays during those months.

4.1.2 Array and system yields

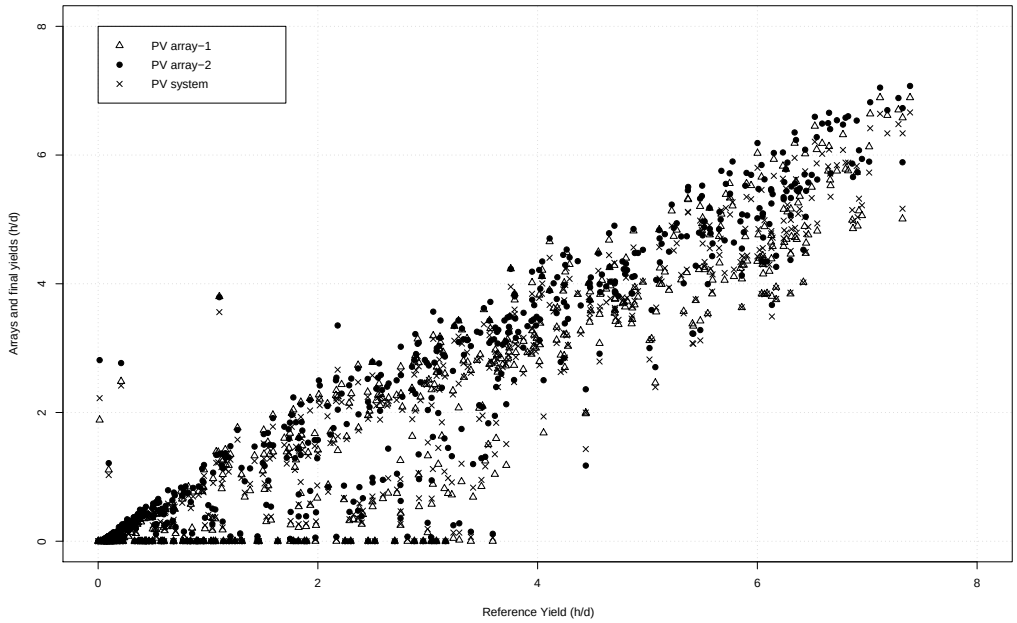

Figure 4.2: PV array and final yields coupled with reference yield during the monitoring period

Daily array and system yields

The daily array and the final yields as a function of the daily reference yield are shown in Fig. 4.2. The daily average PV Array-1, PV Array-2, and final

[2]A descriptive statistics method, more information about boxplot can be found in Wikipedia: http://en.wikipedia.org/wiki/Box_plot

yields over the monitored period were 2.08 h/d, 2.31 h/d, and 2.06 h/d, respectively. The highest daily array and final yields were 6.89 h/d (PV array-1), 7.07 h/d (PV array-2) and 6.66 h/d (PV system), respectively. There were 40 records where the final yields were lower than 1 h/d when daily reference yields were more than 2 h/d. Of those records 83.7 % occurred between February and April during the monitoring period. This was probably due to the snow accumulation on the PV panels. Rest of the records (16.3 %) occurred in September 2006, either because the mounting fault caused cracks in the PV cells that propagated and caused malfunctions in the cell, or because during the maintenance work in September the PV array-1 was disconnected from the system.

Table 4.2: Monthly average of the daily PV array and system yields

Year	Month	PV Array-1	PV Array-2	PV system
		$Y_{a,m}^{(1)}$ (h/d)	$Y_{a,m}^{(2)}$ (h/d)	$Y_{f,m}$ (h/d)
2005	Feb.	0.22	0.40	0.28
2005	Mar.	1.29	1.81	1.42
2005	Apr.	3.74	3.79	3.55
2005	May	4.35	4.37	4.11
2005	Jun.	4.65	4.74	4.42
2005	Jul.	4.57	5.04	4.54
2005	Aug.	2.81	3.16	2.78
2005	Sep.	1.92	2.07	1.86
2005	Oct.	0.73	0.80	0.69
2005	Nov.	0.08	0.09	0.08
2005	Dec.	0.00	0.00	0.00
2006	Jan.	0.00	0.00	0.00
2006	Feb.	0.00	0.00	0.00
2006	Mar.	0.00	0.03	0.01
2006	Apr.	1.70	1.76	1.59
2006	May	3.06	3.46	3.03
2006	Jun.	3.79	4.39	3.83
2006	Jul.	4.19	4.88	4.28
2006	Aug.	3.01	3.33	3.02
2006	Sep.	0.79	1.10	0.87
2006	Oct.	0.33	0.47	0.36
2006	Nov.	0.07	0.12	0.08
2006	Dec.	0.02	0.04	0.03
Annual average		2.08	2.31	2.06

Monthly array and system yields

Table 4.2 summarizes the monthly average of the daily array and final yields over the monitoring period. On monthly average, the range of the final yields was between 0.28 h/d and 4.54 h/d when the inverters were working. The highest average of the daily array and final yields occurred in July 2005. Values from April to August were higher than the values in winter because of higher daily insolation in summer. The monthly averages of the daily final yield values are smaller than those for other PV system studied in Central Finland [45] and in Central or Western European countries [32, 43] during summer time.

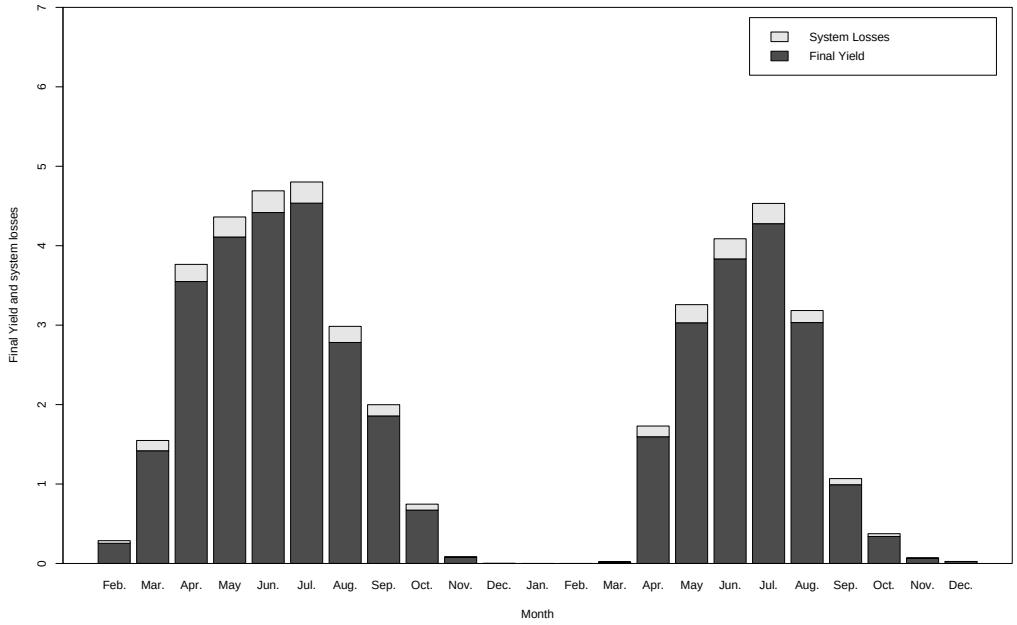

Figure 4.3: Monthly averages of the daily final yield and system losses

4.1.3 System losses

Fig. 4.3 shows the monthly averages of the daily final yield and system losses ($L_{s,m}$). The ratio between average system losses and array yield between October and March was 9.33 % that was higher than the average value 6.76 % between April and September. The higher ratio between average system losses and array yield during winter time may be related to the low performance of inverter under low solar insolation condition. It has been noticed

that the ratio is higher than the value in another PV system study that was also located in Central Finland [45]. The high system losses were due to poor system performance.

4.1.4 Array and system efficiencies

Daily array and system efficiencies

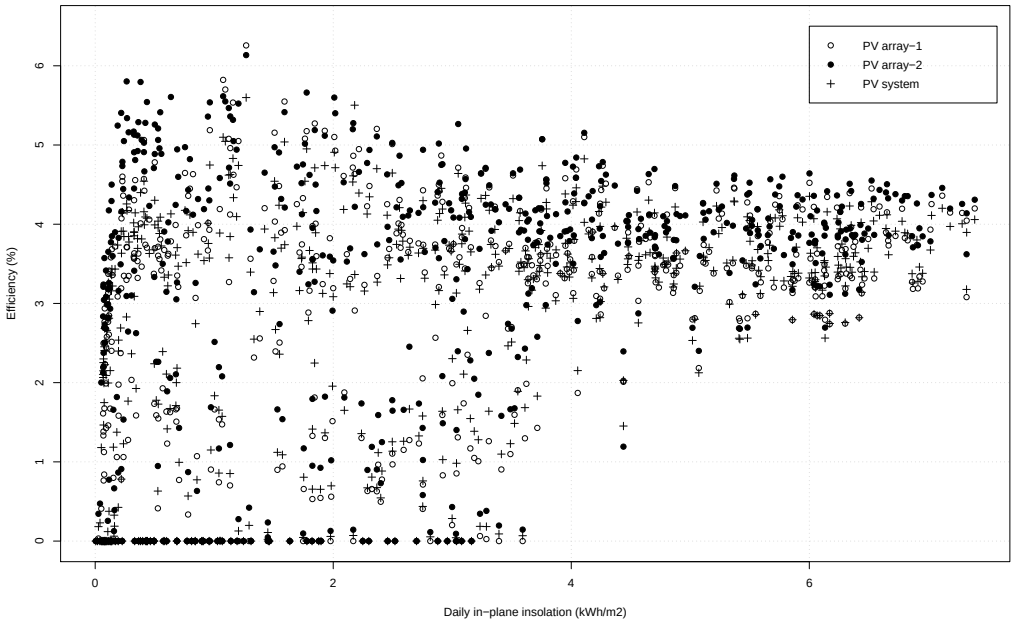

Figure 4.4: PV daily array and system efficiencies coupled with daily total in-plane solar insolation

Fig. 4.4 shows the daily array and system efficiencies as a function of the daily in-plane insolation. The highest efficiency of the PV array-1 ($\eta_{a,d}^{(1)}$), array-2 ($\eta_{a,d}^{(2)}$) and system ($\eta_{s,d}$) was 6.26 %, 6.13 %, and 5.60 %, respectively, and all of these values occurred on 15 June 2006. The averages of the daily efficiency of the PV array-1, array-2, and system were 2.79 %, 3.21 %, and 2.78 %, respectively. The efficiency values were higher in summer than they were in winter, this is due to the strong solar irradiance with relatively low ambient temperature in summer. There were 49 records where the system efficiencies were lower than 2 % when daily reference yields were more than 2 h/d. Of those records 81.6 % occurred between February and April dur-

ing the monitoring period, rest of records (18.4 %) occurred in August and September 2006.

Monthly array and system efficiencies

Table 4.3: PV array and system efficiencies

Year	Month	PV array-1		PV array-2		PV system	
		$\bar{\eta}_{a,m}^{(1)}$ (%)	$\eta_{a,m}^{(1)}$ (%)	$\bar{\eta}_{a,m}^{(2)}$ (%)	$\eta_{a,m}^{(2)}$ (%)	$\bar{\eta}_{s,m}$ (%)	$\eta_{s,m}$ (%)
2005	Feb.	0.94	0.79	1.67	1.41	1.19	0.97
2005	Mar.	1.78	1.89	2.58	2.66	1.98	2.09
2005	Apr.	4.08	3.92	4.11	3.97	3.83	3.72
2005	May	4.78	4.39	4.78	4.41	4.48	4.15
2005	Jun.	4.63	4.47	4.69	4.56	4.36	4.25
2005	Jul.	4.23	4.09	4.66	4.51	4.17	4.06
2005	Aug.	4.08	3.91	4.54	4.39	3.99	3.87
2005	Sep.	3.84	3.61	4.09	3.89	3.64	3.49
2005	Oct.	3.75	3.53	4.05	3.87	3.48	3.32
2005	Nov.	2.03	2.37	2.07	2.42	1.87	2.15
2005	Dec.	0.00	0.00	0.07	0.11	0.03	0.05
2006	Jan.	-	-	-	-	-	-
2006	Feb.	-	-	-	-	-	-
2006	Mar.	0.00	0.00	0.04	0.06	0.02	0.03
2006	Apr.	1.95	2.29	2.08	2.38	1.85	2.16
2006	May	3.24	3.13	3.66	3.54	3.20	3.10
2006	Jun.	3.46	3.40	4.00	3.94	3.48	3.44
2006	Jul.	3.40	3.38	3.95	3.94	3.46	3.45
2006	Aug.	3.35	3.29	3.68	3.64	3.33	3.30
2006	Sep.	2.40	2.09	3.40	2.92	2.65	2.31
2006	Oct.	3.11	2.96	4.58	4.24	3.48	3.26
2006	Nov.	0.95	1.07	1.86	1.92	1.30	1.36
2006	Dec.	0.86	1.17	1.88	2.34	1.30	1.66

Table 4.3 shows the array and system efficiencies calculated using the two methods mentioned in Sec. 2.6.1. By using method two, the monthly efficiencies of the PV array-1, array-2, and system were 2.42 %, 2.83 %, and 2.44 %, respectively. The efficiency values calculated by method two were generally smaller than for method one. We noticed that although the monthly total solar insolation in summer 2006 were higher than in summer 2005, the highest average daily PV array and system efficiency occurred in June 2005, and higher values appeared between May and August 2005. This result may

be explained by the larger number of the malfunctioning PV cells in 2006 than in 2005. Between December 2005 and March 2006, the monthly average efficiencies were approximate zero that was due to the PV system shutdown during the winter because of low solar insolation. The monthly average of the system efficiency is significantly lower than in the earlier studies in other locations all over the world [46, 32, 43, 44, 45, 47, 48]. This result is mainly because lower efficiency PV modules were used in our case, and PV cells malfunctioned during the monitoring period. Several broken PV modules were replaced in September 2006 and hence PV system efficiency increased in October 2006.

4.1.5 Inverter performance

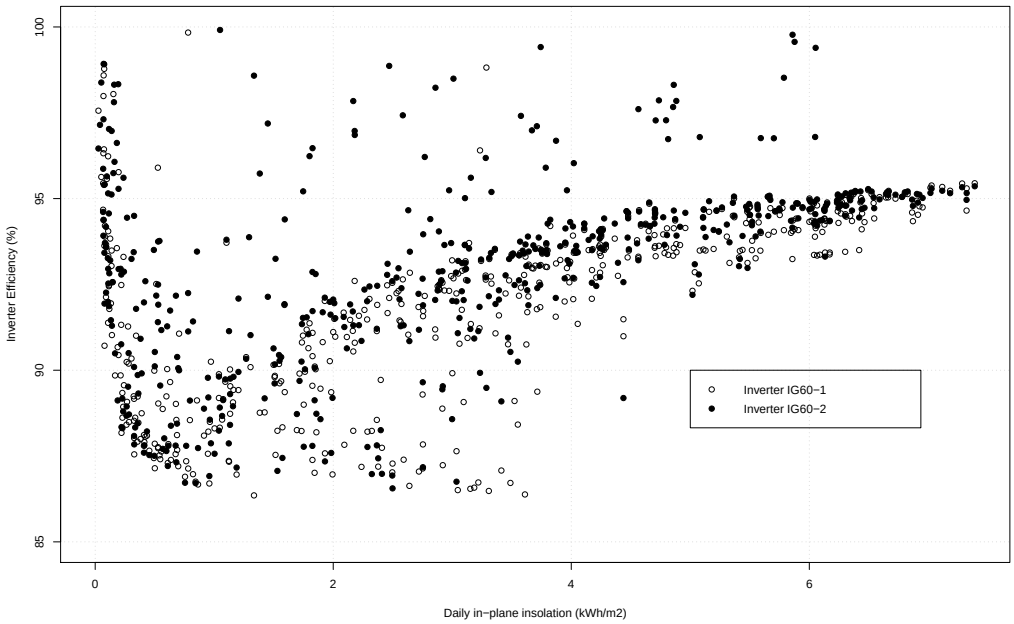

Figure 4.5: Inverters efficiencies

Daily inverter efficiency

Fig. 4.5 shows daily inverter efficiencies as a function of the daily in-plane solar insolarion. Over the monitoring period, the averaged daily inverter efficiency of the IG 60-1 and IG 60-2 was 91.99 % and 92.97 %, respectively.

The daily inverter efficiencies of IG 60-2 were generally higher than the inverter IG 60-1. Although the designed PV array capacity was the same, the broken PV modules in the PV Array-1 made it generate less electricity than the Array-2, this problem caused more power losses and inverter IG 60-1 was actually oversized before the broken PV modules were replaced.

Table 4.4: Inverters efficiencies

Year	Month	IG 60-1		IG 60-2	
		$\bar{\eta}^{(1)}_{inv,m}$ (%)	$\eta^{(1)}_{inv,m}$ (%)	$\bar{\eta}^{(2)}_{inv,m}$ (%)	$\eta^{(2)}_{inv,m}$ (%)
2005	Feb.	90.24	89.22	88.21	87.73
2005	Mar.	89.05	90.85	90.96	92.17
2005	Apr.	93.85	94.26	93.83	94.27
2005	May	93.82	94.22	93.82	94.22
2005	Jun.	93.68	94.17	93.67	94.18
2005	Jul.	93.83	94.38	94.03	94.52
2005	Aug.	92.44	92.97	92.88	93.42
2005	Sep.	91.08	92.03	92.92	93.75
2005	Oct.	89.30	89.57	89.60	90.10
2005	Nov.	-	89.56	-	89.68
2005	Dec.	-	-	-	95.23
2006	Jan.	-	-	-	-
2006	Feb.	-	-	-	-
2006	Mar.	-	96.37	-	92.48
2006	Apr.	-	92.23	91.78	92.15
2006	May	92.37	92.73	92.98	93.37
2006	Jun.	93.15	93.56	93.61	94.00
2006	Jul.	93.92	94.03	94.62	94.67
2006	Aug.	92.65	93.04	96.55	97.13
2006	Sep.	88.95	89.68	92.28	93.82
2006	Oct.	89.01	88.23	92.25	92.38
2006	Nov.	-	90.43	-	91.50
2006	Dec.	-	93.87	-	94.94

Monthly inverter efficiency

Table 4.4 summarizes monthly inverter efficiencies calculated using two methods mentioned in Sec. 2.6.1. Under dark or overcast weather conditions, the PV output was very low, and therefore, the inverters operated at low input conditions. Several months in winter were without any result or with very high inverter efficiency, that because with low DC input, the inverters

could not start operation as its threshold energy level could not be met. The monthly inverter efficiency values were fairly stable for both inverter IG 60-1 and IG 60-2, however, inverter IG 60-2 efficiency values were higher than inverter IG 60-1. Higher values but better efficiency results were obtained by using the method two. During the monitoring period, by using the analysis method two, the monthly inverter IG 60-1 and IG 60-2 efficiencies were 92.27 % and 93.13 %, respectively. Although these results are less than the technical data 93.5 % offered by the manufacturer, considering the broken PV modules made two inverters actually over sized, this result shows that the performance of both inverters was excellent.

4.1.6 Performance Ratio

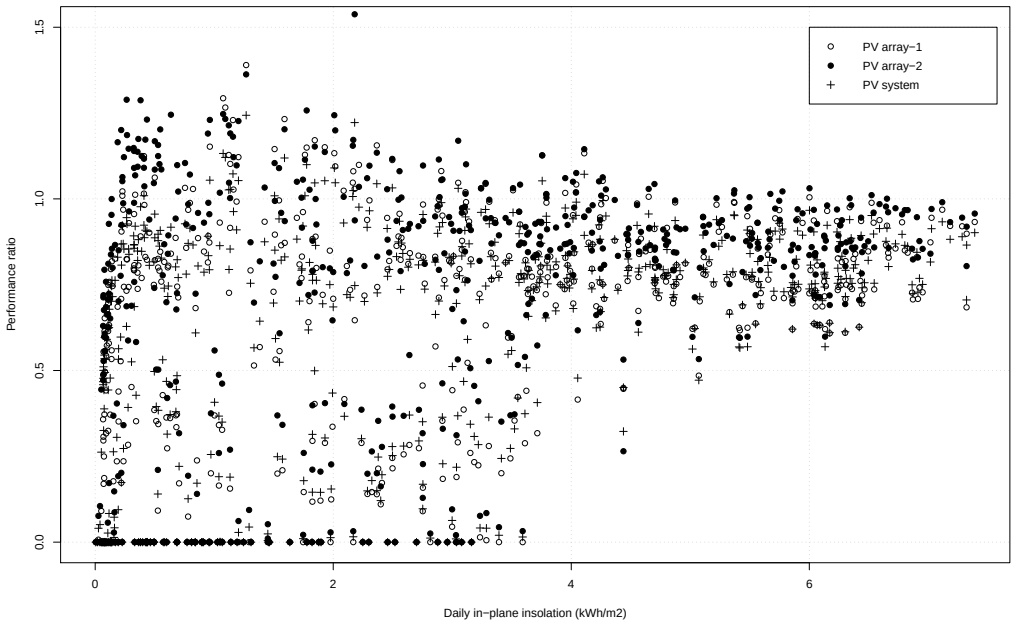

Figure 4.6: Daily PV array and system Performance Ratios

Daily performance ratio

Fig. 4.6 shows daily PV array and system performance ratios as a function of daily in-plane insolation over the monitoring period. The daily PV Array-1, Array-2 and system performance ratios over the monitoring period were 0.620, 0.714, and 0.618, respectively. There were 26 records (as shown with

'+' marks) where the daily PV system Performance Ratios were more than 1.

Monthly performance ratio

Table 4.5 shows the monthly PV array and system performance ratios using the two methods mentioned in Sec. 2.6.1. The range of monthly average system performance ratio was between 0.22 and 0.95 when the inverters were working. Theoretical daily and monthly performance ratio range should be

Table 4.5: Monthly PV array and system Performance Ratios

Year	Month	PV array-1		PV array-2		PV system	
		$\overline{PR}_{a,m}^{(1)}$	$PR_{a,m}^{(1)}$	$\overline{PR}_{a,m}^{(2)}$	$PR_{a,m}^{(2)}$	$\overline{PR}_{s,m}$	$PR_{s,m}$
2005	Feb.	0.21	0.17	0.21	0.31	0.27	0.22
2005	Mar.	0.39	0.42	0.39	0.59	0.44	0.46
2005	Apr.	0.91	0.87	0.91	0.88	0.85	0.83
2005	May	1.06	0.98	1.06	0.98	1.00	0.92
2005	Jun.	1.03	0.99	1.03	1.01	0.97	0.95
2005	Jul.	0.94	0.91	0.94	1.00	0.93	0.90
2005	Aug.	0.91	0.87	0.91	0.97	0.89	0.86
2005	Sep.	0.85	0.80	0.85	0.86	0.81	0.77
2005	Oct.	0.83	0.78	0.83	0.86	0.77	0.74
2005	Nov.	0.45	0.53	0.45	0.54	0.42	0.48
2005	Dec.	0.00	0.00	0.00	0.02	0.01	0.01
2006	Jan.	0.00	0.00	0.00	0.00	0.00	0.00
2006	Feb.	0.00	0.00	0.00	0.00	0.00	0.00
2006	Mar.	0.00	0.00	0.00	0.01	0.00	0.01
2006	Apr.	0.43	0.51	0.43	0.53	0.41	0.48
2006	May	0.72	0.70	0.72	0.79	0.71	0.69
2006	Jun.	0.77	0.75	0.77	0.87	0.77	0.76
2006	Jul.	0.75	0.75	0.75	0.87	0.77	0.77
2006	Aug.	0.74	0.73	0.74	0.81	0.74	0.73
2006	Sep.	0.53	0.46	0.53	0.65	0.59	0.51
2006	Oct.	0.69	0.66	0.69	0.94	0.77	0.72
2006	Nov.	0.21	0.24	0.21	0.43	0.29	0.30
2006	Dec.	0.19	0.26	0.19	0.52	0.29	0.37

between 0 and 1, and PR range is between 0.70 and 0.90 for daily insolation higher than 2 kWh/m^2 as defined in IEC 61724.

In our case, both daily and average monthly PR were rather high, the daily PV array PR value was even larger than 1. These were probably caused

either by the higher energy output that was recorded or the lower solar insolation that was obtained. Since no other instruments were used to monitor the system, we could not check the data we had obtained. The relatively high PR can be explained by the accuracy of the reference solar cell sensor. It was indicated in Ref. [49] that the applied irradiance-calibration can have a significant impact on the long term measurements and on the relative deviations between instantaneous measurements by sensors and pyranometer. In our study, the reference solar cell sensor accuracy offered by the sensor manufacturer was $\pm 5\,\%$ averaged over a year. We believe that the obtained solar insolation data was $5\,\%$ less than the real value on annual basis. In other words, if the accuracy of reference solar cell sensor was considered, the annual average daily solar insolation value might increase $5\,\%$; the PV Array-1, Array-2 and system reference yields, efficiencies, and performance ratios might degrade $5\,\%$, respectively.

4.1.7 Energy output

The manufacturer estimated annual energy output was 3000 kWh.

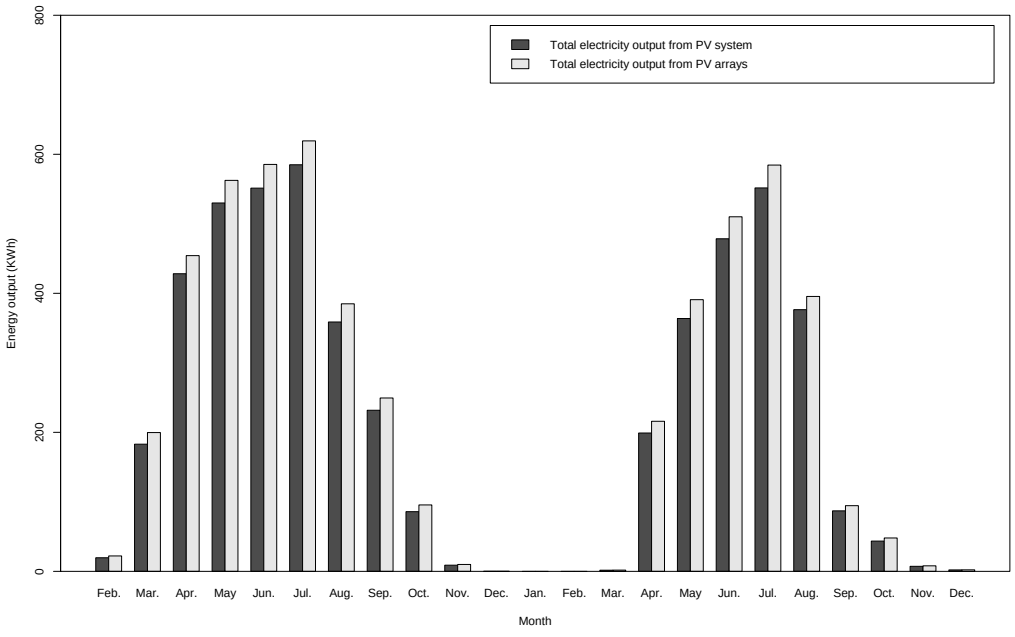

Figure 4.7: Monthly electricity from PV arrays and system

Table 4.6: Monthly arrays and system electricity outputs

Year	Month	PV array-1	PV array-2	PV system
		$E_a^{(1)}$(kWh)	$E_a^{(2)}$ (kWh)	E_s (kWh)
2005	Feb.	7.92	14.25	19.57
2005	Mar.	82.86	116.81	182.95
2005	Apr.	225.61	228.60	428.15
2005	May	280.51	281.97	529.95
2005	Jun.	289.92	295.49	551.31
2005	Jul.	294.57	324.70	584.93
2005	Aug.	181.46	203.44	358.74
2005	Sep.	120.09	129.32	231.76
2005	Oct.	45.59	49.97	85.86
2005	Nov.	4.91	5.01	8.89
2005	Dec.	0.00	0.04	0.04
2006	Jan.	0.00	0.00	0.00
2006	Feb.	0.00	0.00	0.00
2006	Mar.	0.10	1.68	1.64
2006	Apr.	105.89	110.01	199.04
2006	May	183.49	207.35	363.74
2006	Jun.	236.23	273.86	478.44
2006	Jul.	269.95	314.54	551.59
2006	Aug.	187.73	207.76	376.46
2006	Sep.	39.37	55.12	87.02
2006	Oct.	19.75	28.28	43.55
2006	Nov.	2.84	5.10	7.24
2006	Dec.	0.73	1.45	2.06
Total		2579.50	2854.76	5092.93

Daily electricity outputs from arrays and system

The highest daily electricity generated by the PV array-1 and PV array-2 was 14.34 kWh and 14.71 kWh both of which occurred 20 June 2005. The highest daily amount of electricity fed to the grid from PV system was 27.71 kWh which also occurred 20 June 2005. The number of days without electricity output from the PV array-1 was 91 days and from array-2 was 73 days, they were mainly during the winter 2005 and 2006, and also caused by the maintenance work during September 2006.

Monthly electricity outputs from array and system

Table 4.6 shows the monthly total electricity output from the PV arrays and system. Fig. 4.7 shows the monthly arrays and system electricity output. Although the solar insolation in 2006 was more than in 2005, the broken PV modules in PV array-1 made the electricity production in 2006 to be less than 2005. The highest monthly electricity output was 584.93 kWh, that occurred in July 2006 due to the high solar insolation. Total energy output during the monitoring period was 5092.93 kWh, thus, the average daily energy output during the monitoring period was 8.57 kWh. Of the annual electricity production 86.83 % was generated between April and August in 2005 and 2006. The actual enery out put was 84.88 % as estimated output.

4.2 Wind electricity sub-system

The wind energy sub-system analysis was based on the 10 minutes average meteorological data (wind speed and direction) between 1 January 2005 and 31 December 2006. The data recovery rate was 95.5 %. Unfortunately, the wind sub-system data measurement was unreliable. Firstly, the power output and energy production values were not real-time recorded, only the accumulative electricity output values were casually recorded at the end of the month by the energy meter. Secondly, the anemometer was not accurate (when the wind speed less than 1.5 m/s, it will be recorded as 0) and the anemometer accuracy was 5 % on yearly basis. Thirdly, the wind speed and direction accuracy were affected by the turbine blades when they were rotating and by the wind turbine mast.

4.2.1 Yearly and monthly wind characteristics

The average wind speed, shape parameter, scale parameter, most probable wind speed, and wind speed carrying maximum energy on monthly and yearly basis are summarized in Table 4.7.

Wind speed

Fig. 4.8 shows the average wind speeds in 2005 and 2006. The average wind speed over the monitoring period was 3.30 m/s and the highest value of the average monthly wind speed was 4.92 m/s which occurred in December 2006. The maximum wind speed during the monitoring period was 22.3 m/s. The cut-in wind speed of WT-10P wind turbine is 3.50 m/s and considering the average wind speed in Viitasaari, the wind turbine was definitely over-sized.

Table 4.7: Yearly and monthly average wind speed, shape parameter, scale parameter, most probale wind speed, and wind speed carrying maximum energy

Year	Month	Shape parameter k	Scale parameter c (m/s)	Mean wind speed $\overline{V}$ (m/s)	Most probable wind speed V_{mp} (m/s)	Wind speed carrying maximum energy V_{MaxE} (m/s)
2005	Jan.	2.18	3.87	3.39	2.92	5.23
2005	Feb.	1.77	3.91	3.33	2.45	5.99
2005	Mar.	1.75	3.12	2.58	1.92	4.83
2005	Apr.	1.46	3.21	2.83	1.46	5.80
2005	May	1.65	3.95	3.48	2.24	6.40
2005	Jun.	1.93	3.78	3.34	2.60	5.46
2005	Jul.	1.64	2.94	2.59	1.66	4.77
2005	Aug.	1.91	4.37	3.85	2.97	6.36
2005	Sep.	2.08	4.77	4.22	3.48	6.60
2005	Oct.	2.47	4.68	4.06	3.79	5.95
2005	Nov.	2.73	4.85	3.75	4.10	5.94
2005	Dec.	1.42	3.26	2.55	1.39	6.04
Annual		1.78	3.90	3.33	2.46	5.94
2006	Jan.	1.74	3.46	3.01	2.12	5.36
2006	Feb.	1.67	2.90	2.36	1.68	4.64
2006	Mar.	1.07	3.39	3.11	0.27	9.04
2006	Apr.	2.38	3.66	3.20	2.91	4.73
2006	May	1.64	2.95	2.53	1.66	4.79
2006	Jun.	1.96	4.06	3.55	2.82	5.82
2006	Jul.	1.85	3.51	3.03	2.31	5.21
2006	Aug.	1.80	2.96	2.57	1.89	4.47
2006	Sep.	2.20	4.05	3.59	3.07	5.44
2006	Oct.	2.06	3.96	3.51	2.87	5.51
2006	Nov.	1.96	4.27	3.74	2.96	6.12
2006	Dec.	2.23	5.57	4.92	4.26	7.42
Annual		1.68	3.76	3.27	2.19	6.01
2005-06		1.73	3.83	3.30	2.32	5.98

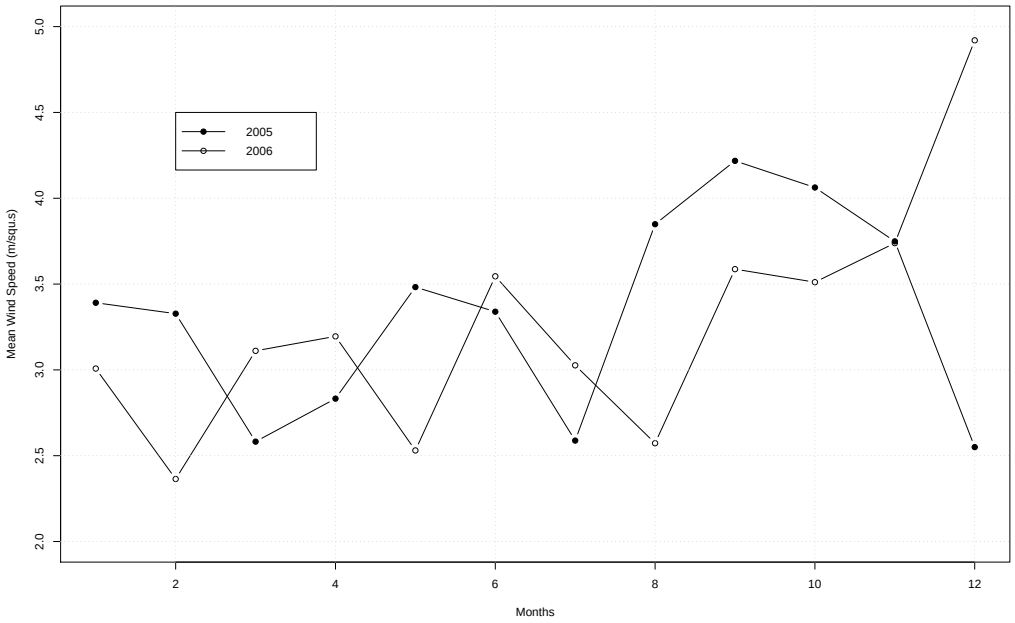

Figure 4.8: Monthly mean wind speed of Year 2005 and 2006

As we know, the wind speed is the key element to indicate the abundance and quality of the wind resource. In Ref. [24], Wind Power Classes were defined in terms of the upper limits of mean wind power density and mean wind speed at 30 m above the ground level (see Table 4.8). The Class 4 or greater locations are generally considered to be suitable for most wind turbine applications, Class 3 areas are suitable for wind energy development using tall turbines, Class 2 areas are marginal and Class 1 areas are unsuitable for wind energy development [24]. In our case the ISS was suited in 31 m height, the Classes of wind power density can be used. We noticed that the anemometer range was from 1.5 to 79 m/s, that means all the wind speeds less than 1.5 m/s were recorded as zero. We believe that the recorded average wind speed should be smaller than the actual wind speed. Although the anemometer accuracy was considered, the actual wind speed still less than 5.1 m/s, therefore, Viitasaari ABC service station can be classified as Class 1 area according to the Wind Power Classes. This means that in 30 m height, the grid-connected wind turbine may be not suitable for Viitasaari area. The wind turbine might receive larger wind speed and perform better in a higher place.

Table 4.8: Classes of wind power density

Wind Power Class	Power Density (W/m^2)	Wind Speed (m/s)
1	≤ 160	≤ 5.1
2	≤ 240	≤ 5.9
3	≤ 320	≤ 6.5
4	≤ 400	≤ 7.0
5	≤ 480	≤ 7.4
6	≤ 640	≤ 8.2
7	≤ 1600	≤ 11.0

Weibull distribution

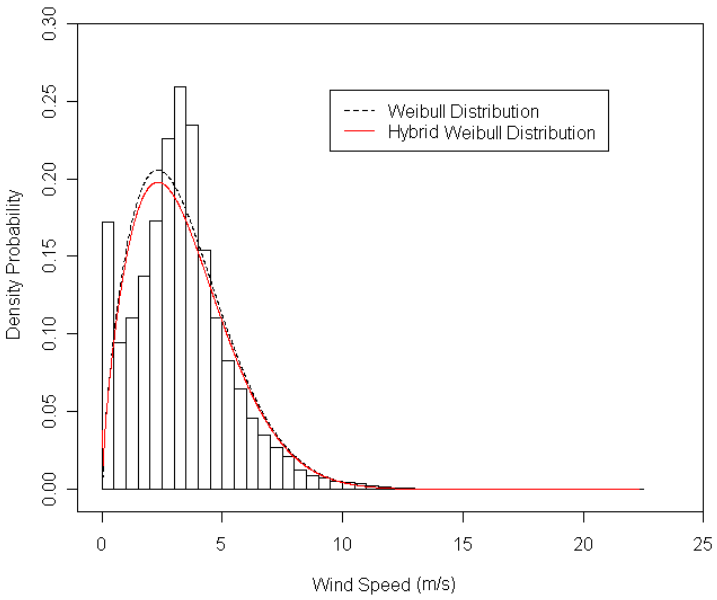

Figure 4.9: Weibull distribution in two methods

In this study, hybrid and normal two parameters Weibull probability density functions were used to express the wind characteristics. Fig. 4.9 and 4.10 show the Weibull and the Cumulative Weibull distributions determined using two methods over the monitoring period. In Fig. 4.9, the annual shape parameter k=1.73 made the curve have a heavy bias to the y-axis which means most days were windless or with very low wind speed. Hybrid Weibull distribution shows the probability when wind speed equals zero, hence it decreased

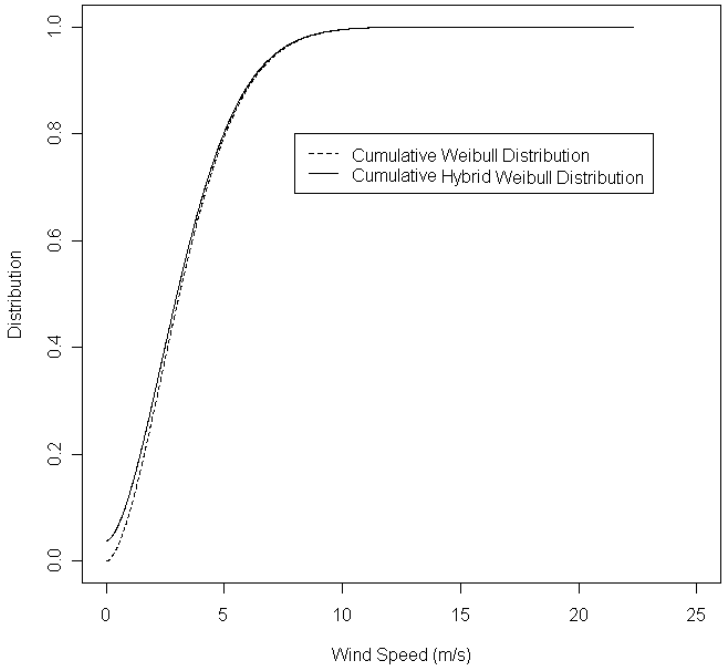

Figure 4.10: Cumulative Weibull distribution in two methods over the monitoring period

other wind speed probabilities. Hybrid Weibull distribution shows a better fitting curve to the hist graphic of the wind speed probability. The range of the monthly shape parameter was between 1.07 and 2.73, and the scale parameter range was between 2.90 and 5.57. The very low shape parameter in March 2006 may be explained by the effect of very high wind speed between 27^{th} to 29^{th}. The highest shape parameter occurred in November 2005. The monthly scale parameters show that they are highly related to the average wind speed.

4.2.2 Wind direction and turbulence intensity

Table 4.9 shows the frequency of different wind directions and the mean wind speed from each direction. The wind directions were measured from the 10 min dominant wind direction. Wind rose maps summarize the occurrence of winds at a location, showing their strength, direction and frequency [50]. Fig. 4.11 shows the wind rose map over the monitoring period. The 12 sectors wind rose was plotted by using Wind Rose Plotter Programme[3]. We

[3]The Wind Rose Plotter Programme was offered by Danish Wind Industry Association. More information can be found: http://www.windpower.org/en/tour/wres/roseplot.htm

Wind directions	Frequency (%)	Mean wind speed (m/s)
E	6.1	3.35
ENE	3.3	3.92
ESE	2.8	3.03
N	10.0	2.23
NE	2.9	3.71
NNE	3.8	4.00
NNW	1.1	1.68
NULL	1.5	0.30
NW	4.6	1.98
S	12.6	3.29
SE	3.5	2.85
SSE	8.2	3.01
SSW	6.5	4.10
SW	4.1	4.14
W	12.1	3.40
WNW	7.2	3.58
WSW	9.6	4.35

Table 4.9: The wind frequency and mean wind speed from each direction

noticed that there was no outstanding wind direction over the monitoring period. The most frequent wind directions were from true south, west and north, and the frequencies from those directions were very closed. The most energy production was carried from western directions. These results might be because North-South direction oriented road next to the site caused a wind tunnel and the wind from the western coast. Fig. 4.12 shows monthly turbulence intensity (TI) over the monitoring period. The TI is a relative indicator of turbulence with low levels indicated by values less than or equal to 0.10, moderate levels to 0.25, and high levels greater than 0.25 [24]. The wind speed standard deviation values in 10 min were I firstly calculated according to the 1 min wind speed data, then divided by 10 min average wind speed, the monthly turbulence intensity then can be calculated by average the 10 min turbulence intensity. In our case, the monthly TI (see Table 4.13 range was between 0.15 and 0.34, and annual site TI was 0.25, the monthly TI values were in moderate and high levels. This result indicates another reason why it is not advisable to install a horizontal axis wind turbine in Viitasaari.

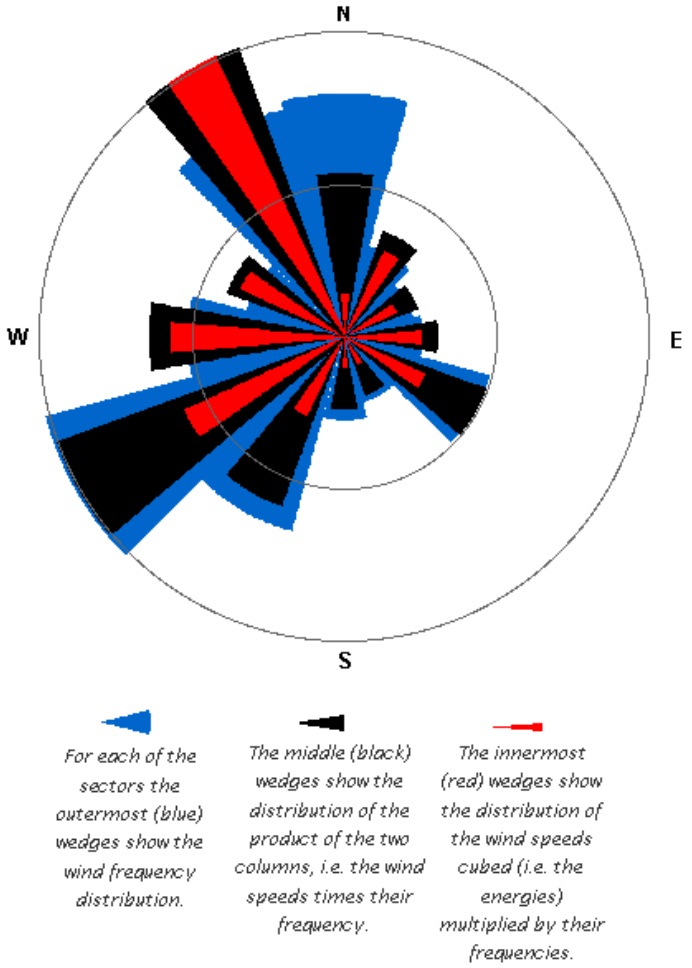

Figure 4.11: 12 sectors wind rose over the monitoring period

4.2.3 Dry and moist air densities

Table 4.10 shows the comparison between dry air and moist air density. We noticed that the range of difference between the dry air and the moist air densities was between 0.001 kg/m^3 and 0.006 kg/m^3 over the monitoring period. On a yearly basis, the difference between the dry air and the moist air densities was only 0.003 kg/m^3. This result indicates that air density is only slightly affected by the vapor in the air in Central Finland region, and thus the dry air density can be used in wind energy analysis. Fig. 4.13 shows the statistical boxplot of the moist air density over the monitoring period. It clearly shows that the air densities during winter were higher than in summer time. As we know, the electricity generated by wind turbine is generally

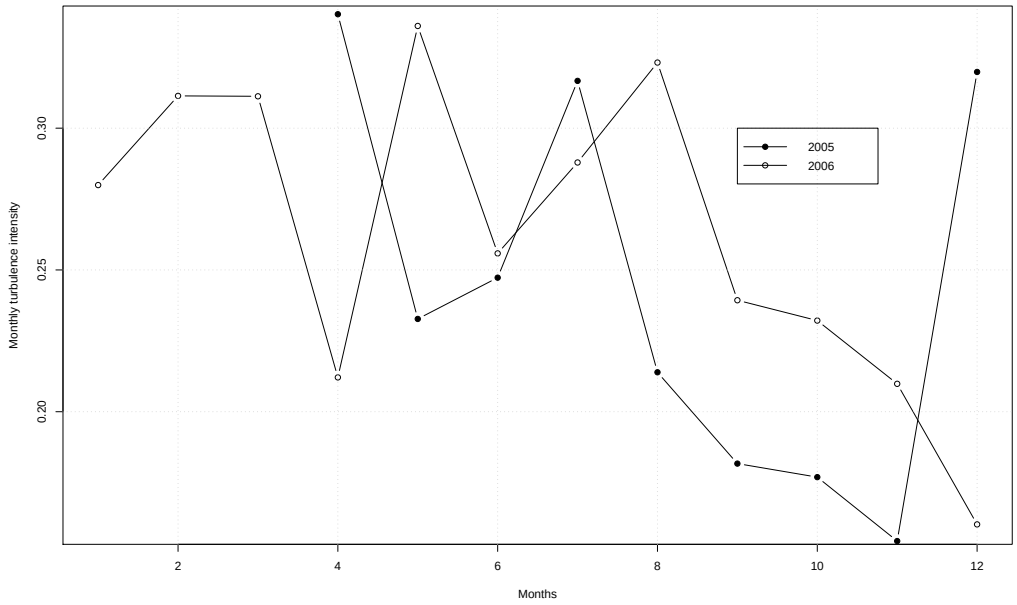

Figure 4.12: Monthly turbulence intensity over the monitoring period

proportional to the air density, and more electricity may be generated in winter because of the higher air density.

4.2.4 Wind power and energy densities

Fig. 4.14 shows the wind power density curves that were calculated using (1) the Weibull distribution coupled with 10 minutes moist air density (PWMD), (2) the Weibull distribution coupled with annual mean moist air density (PWAD), (3) the Hybrid Weibull distribution coupled with 10 minutes moist air density (PHMD) and (4) the Hybrid Weibull distribution coupled with annual mean moist air density (PHAD).

In some studies, the power density was estimated by using annual air density, however, we found that the result is higher than the actual value. We believe that the result may be better fitted by using the Hybrid Weibull distribution coupled with the 10 minutes moist air density (PHMD) method. Table 4.11 shows the annual and monthly power and energy densities. The monthly power density range was between 23.31 W/m^2 and 131.25 W/m^2, the energy density range was between 18.49 kWh/m^2 and 97.65 kWh/m^2. Unfortunately, the monthly power and the energy densities did not show seasonal changes as expected, especially the values in winter were unsatis-

Table 4.10: Dry and Moist air density over the monitoring period

Month	2005		2006	
	Dry air density (kg/m^3)	Moist air density (kg/m^3)	Dry air density (kg/m^3)	Moist air density (kg/m^3)
Jan.	1.303	1.302	1.369	1.368
Feb.	1.339	1.338	1.353	1.353
Mar.	1.329	1.328	1.254	1.253
Apr.	1.275	1.273	1.274	1.272
May	1.250	1.247	1.248	1.245
Jun.	1.226	1.222	1.223	1.219
Jul.	1.207	1.201	1.217	1.212
Aug.	1.219	1.213	1.208	1.202
Sep.	1.240	1.236	1.232	1.227
Oct.	1.272	1.269	1.264	1.261
Nov.	1.270	1.267	1.285	1.283
Dec.	1.322	1.321	1.271	1.269
Annual		1.266		1.263

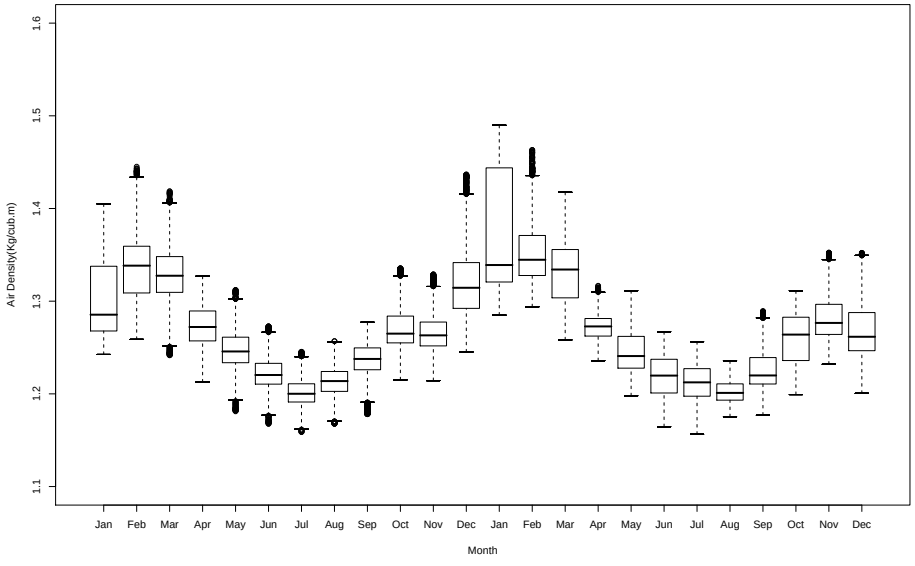

Figure 4.13: Statistical boxplot of moist air density over the monitoring period

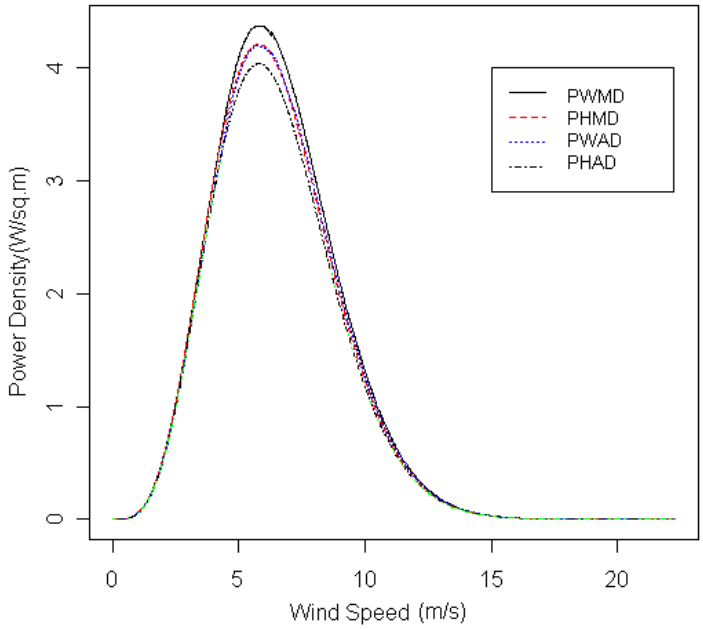

Figure 4.14: Power density curve by using different Weibull distributions and air density values

factory, the wind turbine did not act the major energy contributor in long winter.

4.2.5 Wind energy generated by an ideal and the WT-10P wind turbine

Because of the wind energy production values were not real time measured, the monthly observed electricity values were estimated from the recorded accumulative values. Table 4.12 lists wind electricity generation by an ideal wind turbine and the estimated electricity generation by wind turbine WT-10P, and observed electricity generated by WT-10P. The total observed electricity was only 50.47 % of the total estimated electricity generated by the turbine. We notice the difference between estimated and observed electricity generated by wind turbine WT-10P was significant. Fig. 4.15 expresses the cumulative difference that tended to increase after May 2005. Since the efficiency of the connection electronic box was not given by the manufacturer and no instrument was used to monitor the electricity transformation process between the wind turbine and the grid, there is still no reasonable explanation for this behavior at this point. The electricity quantity difference might be explained by considering icing and high turbulence intensity. As we know,

Table 4.11: Annual and monthly power density and energy density over the monitoring period

Month	2005		2006	
	Power density (W/m^2)	Energy density (kWh/m^2)	Power density (W/m^2)	Energy density (kWh/m^2)
Jan.	46.36	34.49	44.39	33.03
Feb.	61.46	41.30	27.52	18.49
Mar.	31.62	23.52	121.12	90.11
Apr.	44.51	32.05	35.48	25.55
May	65.50	48.73	27.30	20.31
Jun.	45.55	32.79	55.50	39.96
Jul.	26.15	19.45	37.91	28.21
Aug.	70.85	52.71	23.31	17.34
Sep.	85.76	61.74	49.62	35.73
Oct.	72.25	53.75	50.54	37.60
Nov.	75.71	54.51	68.07	49.01
Dec.	50.82	37.81	131.25	97.65
Annual	57.18	500.87	56.07	491.17
2005–2006		56.54		990.58

estimated electricity output mainly depends on the wind speed, however, the wind blew from different directions. The turbulence made the turbine rotor frequently adjust its angle, plus the ice or snow made the turbine yaw even more difficult, therefore, half electricity might be wasted during the adjustment.

Table 4.12: Yearly and monthly electricity generated by an ideal wind turbine, estimated and observed electricity generated by wind turbine WT-10P

Year	Month	Electricity generated by an ideal wind turbine	Estimated Electricity generated by WT-10P	Actual Electricity generated by WT-10P
2005	Jan.	547.34	201.87	266.67
2005	Feb.	836.44	352.03	292.06
2005	Mar.	345.47	114.82	152.38
2005	Apr.	632.93	272.43	184.13
2005	May	1052.79	485.82	247.62
2005	Jun.	607.56	260.05	95.24
2005	Jul.	305.12	112.58	165.08
2005	Aug.	1173.98	563.71	133.33
2005	Sep.	1442.25	694.82	152.38
2005	Oct.	1091.56	492.02	190.48
2005	Nov.	951.27	430.25	253.97
2005	Dec.	666.80	281.27	228.57
2006	Jan.	594.24	224.17	50.79
2006	Feb.	252.71	77.42	76.19
2006	Mar.	1462.13	626.42	120.63
2006	Apr.	280.62	67.60	82.54
2006	May	310.70	111.13	120.63
2006	Jun.	802.94	365.94	114.29
2006	Jul.	476.27	194.02	177.78
2006	Aug.	227.02	66.17	139.68
2006	Sep.	625.72	262.66	126.98
2006	Oct.	696.77	290.88	120.63
2006	Nov.	1049.83	469.74	298.41
2006	Dec.	2426.82	1171.34	342.86
Total		18859.28	8189.16	4133.33

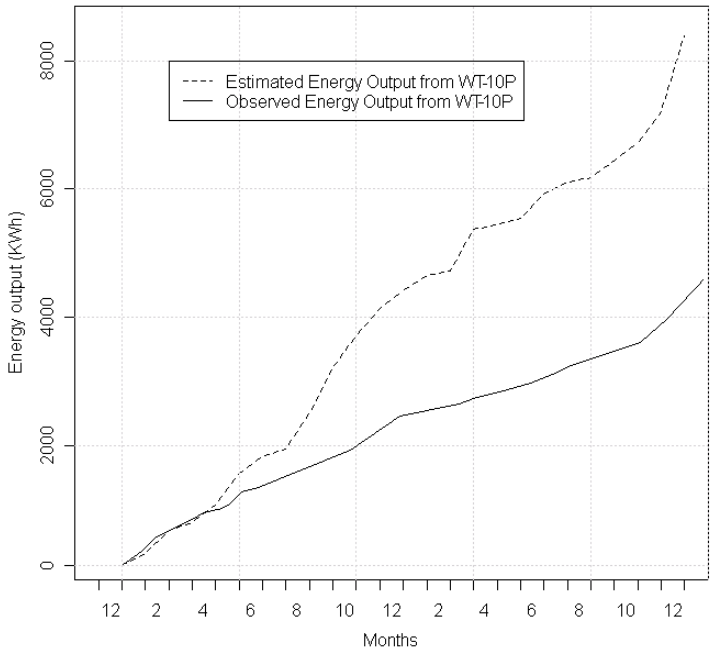

Figure 4.15: Estimated and observed electricity generated by wind turbine WT-10P

4.2.6 Wind turbine efficiency, capacity factor and wind availability factor

Table 4.13 summarizes yearly and monthly average wind speed, wind turbine efficiency, capacity factor, and wind availability factor, site turbulence intensity and data recovery rate over the monitoring period. The wind turbine efficiency ranged between 0.29 and 0.48, and the annual average efficiency was 0.44. The turbine efficiency is acceptable considering the low wind speed area. There is no evidence that the efficiency is significantly correlated to the turbulence intensity as we assumed. The capacity factor range was between 0.01 and 0.16, and the annual average capacity factor was 0.05. This result indicates that the wind turbine WT-10P is over-sized for the Central Finland region. The wind availability factor range was from 0.16 to 0.34, and the two years wind availability factor was 0.42. This means in 58 % of the monitoring period, the wind speed was less than the turbine's cut-in wind speed, the turbine's cut-in wind speed is obviously too high for Viitasaari. None of these factors shows tendency of seasonal variation, indicating that the wind sub-system might not generate electricity consistently on a seasonal basis.

Table 4.13: Yearly and monthly average wind speed, wind turbine efficiency, capacity factor, and wind availability factor, site turbulence intensity and data recovery rate over the monitoring period

Year	Month	Mean wind speed	Wind turbine efficiency	Capacity factor	Wind Availability factor	Turbulence intensity	Data recovery rate
2005	Jan.	3.39	0.37	0.03	0.49	-	0.72
2005	Feb.	3.33	0.42	0.05	0.45	-	0.99
2005	Mar.	2.58	0.33	0.02	0.27	-	0.99
2005	Apr.	2.83	0.43	0.04	0.29	0.34	0.98
2005	May	3.48	0.46	0.07	0.37	0.23	0.98
2005	Jun.	3.34	0.43	0.04	0.41	0.25	1.00
2005	Jul.	2.59	0.37	0.02	0.24	0.32	1.00
2005	Aug.	3.85	0.48	0.08	0.48	0.21	1.00
2005	Sep.	4.22	0.48	0.10	0.62	0.18	1.00
2005	Oct.	4.06	0.45	0.07	0.63	0.18	1.00
2005	Nov.	3.75	0.45	0.06	0.60	0.15	1.00
2005	Dec.	2.55	0.42	0.04	0.30	0.32	1.00
Annual		3.33	0.44	0.05	0.43	0.24	0.97
2006	Jan.	3.01	0.38	0.03	0.40	0.28	0.54
2006	Feb.	2.36	0.31	0.01	0.25	0.31	1.00
2006	Mar.	3.11	0.43	0.08	0.33	0.31	0.98
2006	Apr.	3.20	0.24	0.01	0.39	0.21	1.00
2006	May	2.53	0.36	0.01	0.22	0.34	0.92
2006	Jun.	3.55	0.46	0.05	0.48	0.26	1.00
2006	Jul.	3.03	0.41	0.03	0.32	0.29	1.00
2006	Aug.	2.57	0.29	0.01	0.23	0.32	1.00
2006	Sep.	3.59	0.42	0.04	0.49	0.24	0.83
2006	Oct.	3.51	0.42	0.04	0.50	0.23	1.00
2006	Nov.	3.74	0.45	0.07	0.50	0.21	1.00
2006	Dec.	4.92	0.48	0.16	0.72	0.16	1.00
Annual		3.27	0.44	0.05	0.40	0.26	0.94
2005–2006		3.30	0.44	0.05	0.42	0.25	0.96

4.3 Hybrid PV and Wind Electricity Generation System

Table 4.14 and Fig. 4.16 show the electricity generated by the wind turbine WT-10P and the PV system. Over the monitoring period, the total electricity production was 8962.64 kWh, and the range of the monthly electricity production was between 50.79 kWh (January 2006) and 777.57 kWh (May 2005). Of the total electricity 43.14 % was generated by wind turbine WT-10P and 56.86 % was generated by the PV arrays. The estimated annual HPWS electricity production was 7.09 MWh(PV system: 3 MWh and wind turbine: 4.09 MWh), if the estimated values can be reached, the total electricity production will increase 5226.5 kWh. The grid connected Hybrid PV and Wind Electricity Generation System did not supply a reliable and consistent energy production during the monitoring months in Central Finland Region.

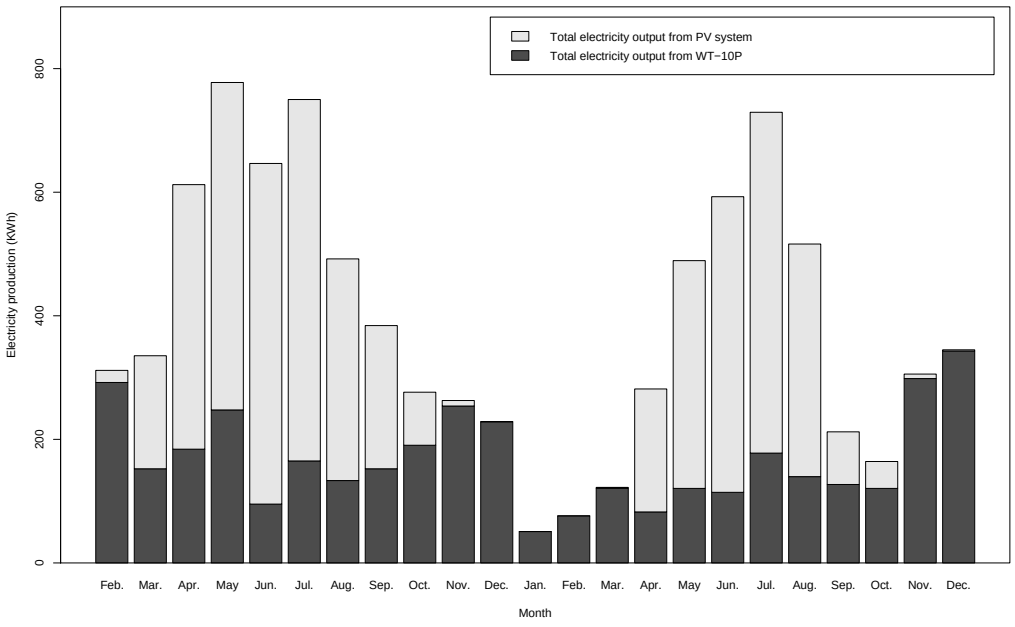

Figure 4.16: Electricity generated by wind turbine WT-10P, PV system, and HPWS

Table 4.14: Electricity generated by wind turbine WT-10P, PV system, and HPWS

Year	Month	Electricity generated by WT-10P (kWh)	Electricity generated by PV system (kWh)	Electricity generated by HPWS (kWh)
2005	Feb.	292.06	19.57	311.63
2005	Mar.	152.38	182.95	335.33
2005	Apr.	184.13	428.15	612.28
2005	May	247.62	529.95	777.57
2005	Jun.	95.24	551.31	646.55
2005	Jul.	165.08	584.93	750.01
2005	Aug.	133.33	358.74	492.08
2005	Sep.	152.38	231.76	384.14
2005	Oct.	190.48	85.86	276.34
2005	Nov.	253.97	8.89	262.86
2005	Dec.	228.57	0.04	228.61
2006	Jan.	50.79	0.00	50.79
2006	Feb.	76.19	0.00	76.19
2006	Mar.	120.63	1.64	122.28
2006	Apr.	82.54	199.04	281.58
2006	May	120.63	368.62	489.26
2006	Jun.	114.29	478.44	592.73
2006	Jul.	177.78	551.59	729.37
2006	Aug.	139.68	376.46	516.14
2006	Sep.	126.98	85.18	212.17
2006	Oct.	120.63	43.55	164.18
2006	Nov.	298.41	7.24	305.65
2006	Dec.	342.86	2.06	344.91
Average		168.12	221.56	389.68
Total		3866.67	5095.97	8962.64

Chapter 5

Conclusions

A Hybrid Photovoltaic and Wind Electricity Generation System has been monitored and analyzed over a period of two years at Central Finland in order to examine the behavior of grid-connected hybrid system in cold climate. The monitoring results showed that the grid connected hybrid system is more reliable than the single renewable resource power system. To operate in cold climate improved the PV sub-system efficiency but the icing and snow might decrease the wind energy production. However, the hybrid system in our case did not offer consistent electricity production in Central Finland region and the system performance was unsatisfactory. The PV sub-system performance was affected by the mounting fault that caused cracks on PV modules; the system performance was barely adequate from April to September, and it was affected significantly during the winter months due to operation under low insolation condition and snow accumulation. The wind turbine was oversized, and the turbine performance was unsatisfactory due to low wind speed, icing and high turbulence intensity.

The analysis results were significantly affected by monitoring system accuracy. Better accuracy monitoring instruments and monitoring system design need to be applied for further research.

Even though the utilization of the Grid Connected Hybrid Photovoltaic and Wind Electricity Generation System is limited by the specific site condition, high initial investment, and long pay back period, as the PV and wind energy technology development and financial incentives from the government, the building-integrated HPWS may be applied in near future.

Bibliography

[1] K. Burges *et al.* Terschelling Hybrid System Research - Final Report. Technical Report Joule contract JOU2-CT92-0222, Ecofys, Utrecht, 1995.

[2] Loois G. and B. Van Hemert. Stand-alone Photovoltaic Applications: Lessons Learned. Technical Report IEA-PVPS Task III, James & James (Science Publishers), 1999.

[3] Erik H. Lysen. The International Energy Agency PVPS programme, PV hybrids and the future. In *PV Hybrid Power Systems Conference*, 2000.

[4] A. Rajendra Prasada and E. Natarajanb. Optimization of Integrated Photovoltaicwind Power Generation Systems With Battery Storage. *Energy*, 31:1943–1954, 2006.

[5] International Electrotechnical Commission. Photovoltaic system performance monitoring-guidelines for measurements, data exchange and analysis. Technical Report IEC 61724, International Electrotechnical Commission, 1998.

[6] International Electrotechnical Commission. Wind turbines - Part 12-1: Power performance measurements of electricity producing wind turbines. Technical Report IEC 61400-12-1, International Electrotechnical Commission, 2005.

[7] Michael Ross and Jimmy Royer. *Photovoltaics in Cold Climates*, pages 3–4. James & James (Science Publishers) Ltd., London, 1999.

[8] Michael Ross and Jimmy Royer. *Photovoltaics in Cold Climates*, pages 73–75. James & James (Science Publishers) Ltd., London, 1999.

[9] NREL. Photovoltaics. http://www.nrel.gov/learning/re_photovoltaics.html, July 2007.

[10] Michael Ross and Jimmy Royer. *Photovoltaics in Cold Climates*, page 15. James & James (Science Publishers) Ltd., London, 1999.

[11] Lawrence L. Kazmerski. Solar Photovoltaics R&D at the Tipping Point: A 2005 Ttechnology Overview. *Journal of Electron Spectroscopy and Related Phenomena*, 150:105–135, 2006.

[12] NREL. Wind Energy Basics. http://www.nrel.gov/learning/re_wind.html, July 2007.

[13] Gilbert M. Masters. *Renewable and Efficient Electric Power Systems*, page 310. John Wiley & Sons, Incorporated., Hoboken, NJ, USA, 2004.

[14] Miguel Alonso Abella and F. Chenlo. Choosing the Right Inverter for Grid-Connected PV Systems. *Renewable Energ World*, March-April, 2004.

[15] Donna Munro. Inside Inverters-How They Work, and What is on the Market. *Renewable Energ World*, January-February:89–97, 2006.

[16] Bengt Tammelin, Alain Heimo, and Michel Leroy. Meteorological measurements under icing conditions Eumetnet SWS II project. Technical Report 2001:6, FMI, 2001.

[17] Michael Ross and Jimmy Royer. *Photovoltaics in Cold Climates*, page 107. James & James (Science Publishers) Ltd., London, 1999.

[18] Michael Ross and Jimmy Royer. *Photovoltaics in Cold Climates*, pages 39–45. James & James (Science Publishers) Ltd., London, 1999.

[19] Gilbert M. Masters. *Renewable and Efficient Electric Power Systems*, page 476. John Wiley & Sons, Incorporated., Hoboken, NJ, USA, 2004.

[20] T. Laakso, H. Holttinen, G. Ronsten, L.Tallhaug, R. Horbaty, I. Baring-Gould, A. Lacroix, E. Peltola, and B. Tammelin. State-of-the-art of Wind Energy in Cold Climates. Technical report, IEA, 2003.

[21] Timo Laakso. Wind Energy Projects In Cold Climates. Technical report, IEA, 2005.

[22] International Electrotechnical Commission. Electrical installations of buildings - Part 7-712: Requirements for special installations or locations - Solar photovoltaic (PV) power supply systems. Technical Report IEC 60364-7-712, International Electrotechnical Commission, 2002.

[23] BRE, EA Technology, Halcrows, and Sundog. Photovoltaics in Buildings - Guide to the installation of PV system. Technical Report ETSU S/P2/00355/REP/1, DTI, 2002.

[24] AWS Scientific Inc. Wind Resource Assessment Handbook. Technical Report TAT-5-15283-01, NREL, 1997.

[25] F.Van Hulle. Small Wind Turbine Safety. Technical Report IEC 61400-2, International Electrotechnical Commission, 1994.

[26] IEA. IEA Wind Task II Recommended Practices. http://www.ieawind.org/Task_11/Task_11_RecPractices.html, August 2007.

[27] G. Blaesser and D. Munro. Guidelines for the assessment of photovoltaic plants document B: analysis and presentation of monitoring data. Technical Report EUR 16339EN, JOINT RESEARCH CENTER, European Commission Institute for Systems Engineering and Informatics, 1998.

[28] John A. Duffie and William A. Beckman. *Solar Engineering of Thermal Processes*, page 11. John Wiley & Sons, Incorporated., New York, 1991.

[29] M.Kolhe, K.Agbossou, J. Hamelin, and T.K. Bose. Analytical model for predicting the performance of photovoltaic array coupled with a wind turbine in a stand-alone renewable energy system based on hydrogen. *Renewable Energ*, 28:727–742, 2003.

[30] John A. Duffie and William A. Beckman. *Solar Engineering of Thermal Processes*, pages 83–84. John Wiley & Sons, Incorporated., New York, 1991.

[31] G. Blaesser. PV System Measurements and Monitoring: The European Experience. *Solar Energy Materials and Solar Cells*, 47:167–176, 1997.

[32] Jayanta Deb Modeol, Yigzaw Yohanis, Mervyn Smyth, and Brian Norton. Long Term Performance Analysis of a Grid Connected Photovoltaic System in Northern Ireland. *Energy Conversion and Management*, 47:2925–2947, 2006.

[33] Tsang-Jung Chang, Yu-Ting Wu, Hua-Yi Hsu, Chia-Ren Chu, and Chun-Min Liao. Assessment of Wind Characteristics and Wind Turbine Characteristics in Taiwan. *Renewable Energy*, 28:851–871, 2003.

[34] E.S. Takle and J.M. Brown. Note on the Use of Weibull Statistics to Characterize Wind-Speed Data. *Journal of applied meteorology*, 17:556–559, 1978.

[35] J.V. Seguro and T.W. Lambert. Modern Estimation of the Parameters of the Weibull Wind Speed Distribution for Wind Energy Analysis. *Journal of wind engineering and industrial aerodynamics*, 85:75–84, 2000.

[36] R.S. Davis. Equation for the determination of the density of moist air (1981/91). *Metrologia*, 29:67–70, 1992.

[37] SCHOTT Solar. *ASITHRU thin-film slar module, semitransparent, ASITHRU-30-SG.*

[38] Fronius International GMBH. *FRONIUS IG 15/20/30/40/60/60HV Operating Instructions.*

[39] WINDTOWER DEUTSCHLAND. *WT 10P Technical Data Sheet. Parallel source with the distribution grid 230/400V 50Hz.*

[40] Davis Instruments. *Cabled Vantage Pro2^{TM} and Vantage Pro2 Plus^{TM} Station,6152C,6162C.*

[41] Davis Instruments. *Vantage Pro2^{TM} Console Manual.*

[42] Fronius International GMBH. *PV System Monitoring for FRONIUS IG Inverter Series.*

[43] B. DECKER and U. JAHN. Performance of 170 grid connected PV plants in Northern Germany: Analysis of yields and optimization potentials. *Solar Energy*, 59:127–133, 1997.

[44] S.M. Pietruszko and M. Gradzki. Performance of a grid connected small PV system in Poland. *Applied Energy*, 74:177–184, 2003.

[45] D. Yang and J. Maunuksela. Performance Analysis of a Grid Connected Photovoltaic System in Central Finland. Master's Degree Programme in Renewable Energy, University of Jyväskylä.

[46] Sidrach de Cardona M. and Mora López Ll. Performance Analysis of a Grid-connected Photovoltaic System. *Energy*, 24:93–102, 1999.

[47] Somchai Chokmaviroja, Rakwichian Wattanapongb, and Yammen Suchartc. Performance of a 500 kWP grid connected photovoltaic system at Mae Hong Son Province, Thailand. *Renewable Energy*, 31:19–28, 2006.

[48] Jung Hun Soa, Young Seok Junga, Gwon Jong Yua, Ju Yeop Choib, and Jae Ho Choic. Performance results and analysis of 3 kW grid-connected PV systems. *Renewable Energy*, 32:1858–1872, 2007.

[49] Alexander Storch and Jan Schindl. Irradiance sensors for solar systems. Technical report, Osterreichisches Forschungs- und Prufzentrum Arsenal GesmbH.

[50] Bureau of Meteorology Australian Government. Wind Roses. http://www.bom.gov.au/climate/averages/wind/wind_rose.shtml, July 2007.

Appendix A

The PV arrays wiring scheme

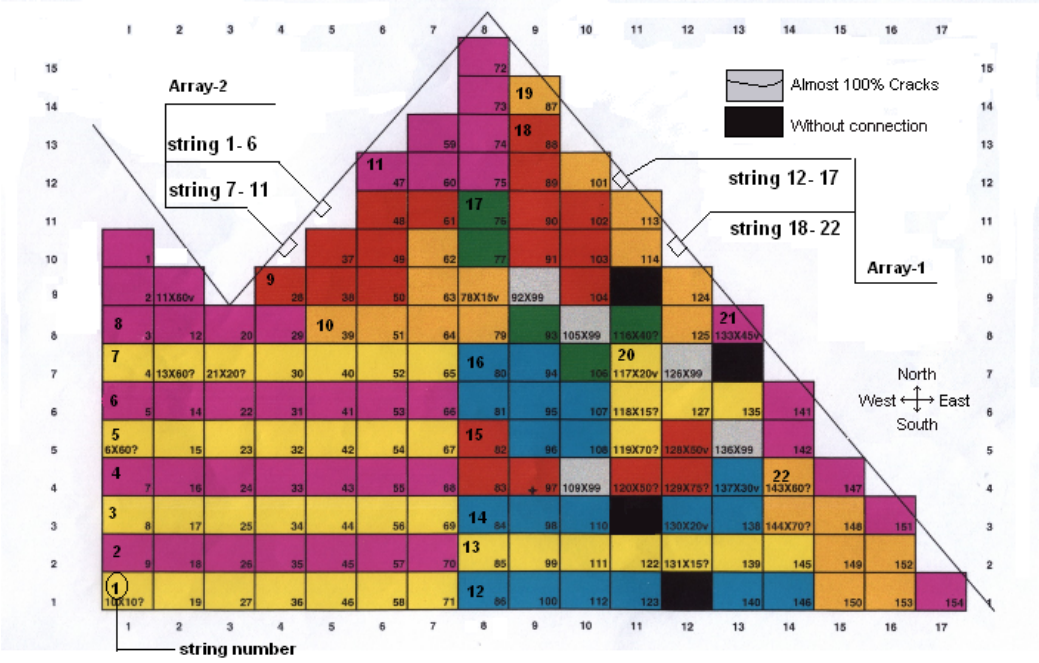

Appendix B

Wind turbine electronic box

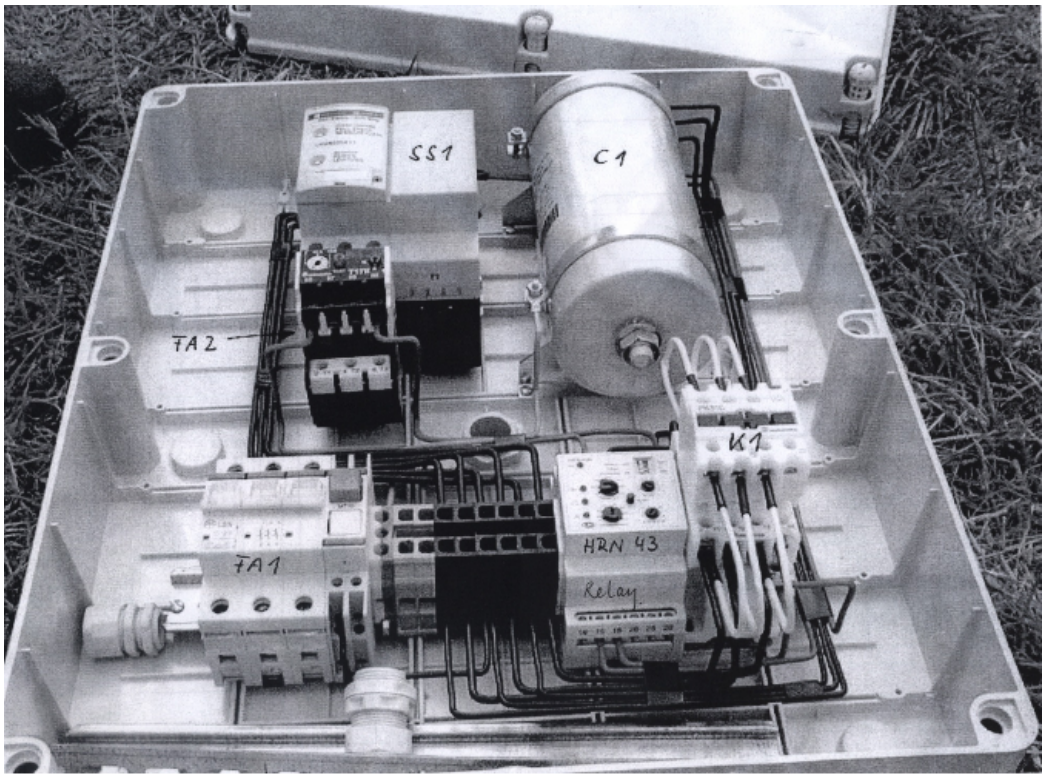

Appendix C

Wind turbine wiring scheme

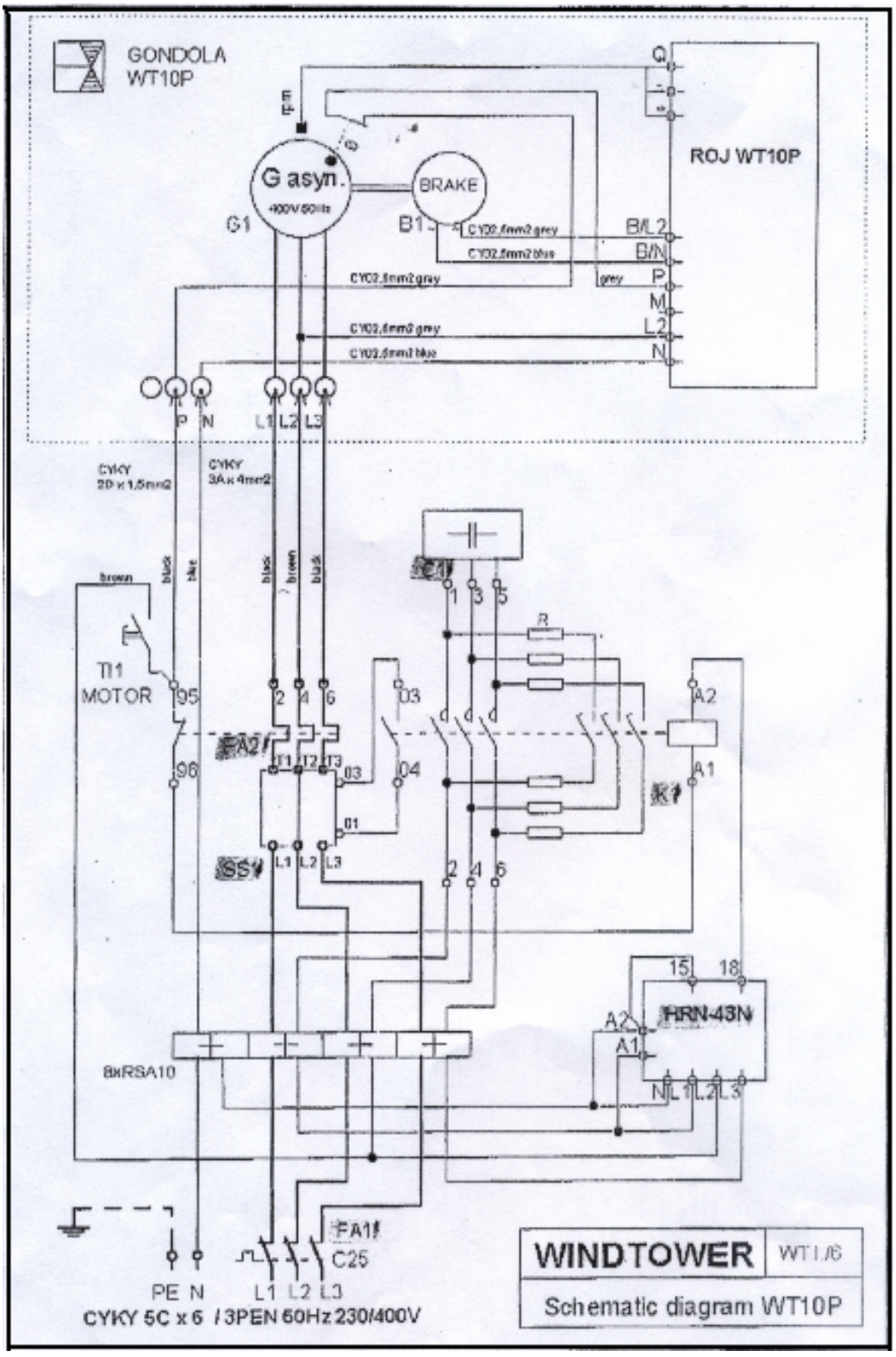
GONDOLA
WT10P
G asyn.
BRAKE
G1
B1
ROJ WT10P
B/L2
B/N
P
M
L2
N
CYKY 2D x 1,5mm2
CYKY 3A x 4mm2
brown
black
blue
TI1
MOTOR
95
96
FA2
K1
A2
A1
15
18
HRN-43N
8xRSA10
FA1
C25
PE N
L1 L2 L3
CYKY 5C x 6 / 3PEN 60Hz 230/400V
WINDTOWER
WT1.0
Schematic diagram WT10P